

Unifying information propagation models on networks and influence maximisation

Yu Tian* and Renaud Lambiotte†

Mathematical Institute, University of Oxford, Oxford, OX2 6GG, United Kingdom

(Dated: May 3, 2022)

Information propagation on networks is a central theme in social, behavioural, and economic sciences, with important theoretical and practical implications, such as the influence maximisation problem for viral marketing. Here, we consider a model that unifies the classical independent cascade models and the linear threshold models, and generalise them by considering continuous variables and allowing feedback in the dynamics. We then formulate its influence maximisation as a mixed integer nonlinear programming problem and adopt derivative-free methods. Furthermore, we show that the problem can be exactly solved in the special case of linear dynamics, where the selection criteria is closely related to the Katz centrality, and propose a customised direct search method with local convergence. We then demonstrate the close-to-optimal performance of the customised direct search numerically on both synthetic and real networks.

I. INTRODUCTION

The rapid growth of online social networks, such as Facebook and Twitter, allows hundreds of millions of people worldwide to interact with each other, providing access to a vast source of information on an unprecedented scale. The *propagation* of information, opinion, innovation, rumour, etc., is a critical component to explain, e.g., how a piece of information could quickly become pervasive through a network via “word-of-mouth” [1–3]. Accordingly, understanding how information spreads in social networks is a central theme in social, behavioural, and economic sciences, with theoretical and practical implications, such as the adoption of political viewpoints in presidential elections and the *influence maximisation* problem for viral marketing [4–6], attracting expertise from various fields including mathematics, physics, and biology [7–9].

Specifically in the context of influence maximisation, one can distinguish two main classes of information propagation models: the independent cascade (IC) model, and the linear threshold (LT) model, where nodes adapt their behaviour from each neighbour independently, or from the collective influence of the whole neighbourhood, respectively [10, 11]. It is well known that both models, which we refer to as “classic models”, suffer from limitations. First of all, the state space of both models is binary, as nodes can only have states either active or not, while various levels of influence and of confidence could co-exist among agents in real cases. Moreover, there is no feedback in both processes, as nodes can only stay active after being activated, thus may not influence back nodes that influenced them as in real life. These limits have called, and still call for more general models allowing us to consider dynamics with feedback between states and more heterogeneity in the agents’ behaviour.

In parallel to this line of work, simple and complex contagions have attracted much research interests in mathe-

matical sociology and physics [12, 13]. Essentially, complex contagion considers situations when the reinforcement of a signal favours its future adoption, which can be modelled via deterministic threshold models. However, their focus is usually on understanding the effects of specific structures, the presence of long ties or the density of triangles for example, and they also tend to consider binary state variables. For models with continuous variables, more has been done within the field of opinion dynamics, where linear models build on the heat equation [14], such as the DeGroot model [15], and nonlinear models include the bounded confidence model for example [16]. A first contribution of this work is to introduce a non-linear, deterministic model for information propagation which relaxes the constraints of binary variables while allowing feedback between states, and also possesses the classic models as limiting cases, thus providing a unifying framework for the information propagation.

As a second contribution, we consider the important problem of influence maximisation (IM), known to have potential applications in various domains [6, 17, 18]. Given a network and an associated information propagation process, the classic IM problem consists in selecting a small set of nodes to activate initially with the aim of maximising the overall influence spread, commonly defined as the number of activated nodes at the end of the process. Kempe et al. [10] formulated it as a stochastic combinatorial optimisation under the classic models, and proposed a greedy algorithm with theoretical approximation guarantees. The near-optimal asymptotic bounds of this seminal work has triggered a vast amount of research in this direction, mostly to further reduce the running time [17, 19]. There are also heuristic solutions, such as centrality-based methods and genetic algorithms, but without theoretical guarantees of the performance [20].

The aforementioned theoretical guarantees are obtained under the assumption that the influence spread is a submodular function, which could be strict in practice [21], and even for the LT model, occurs only for specific choice of the thresholds’ distribution. The IM problem when the thresholds are given by distributions other than

* yu.tian@maths.ox.ac.uk

† renaud.lambiotte@maths.ox.ac.uk

the uniform distribution is relatively unknown. To consider a general information propagation model, we have thus developed a new framework, where we formulate the IM problem as a *mixed integer nonlinear programming* (MINLP). The exact methods for MINLP are mostly based on branch-and-bound plus convex programming, and require first-order information [22–24], which is not generally available in the IM problem. For this reason, we treat the objective function as a black box and adopt *derivative-free methods* [23], with a *mesh adaptive direct search* method as a general solution [25]. Furthermore, we propose a customised method with local convergence, specifically designed for the proposed general class of information propagation model.

The primary goal of our paper is to address the aforementioned drawbacks of the two classic information propagation models, the IC model and the LT model, while maintaining the widely accepted mechanisms underlying both models. With the research interests in simple and complex contagions taken into consideration, we extend both classic models for continuous state variables while allowing feedback between states in the deterministic case, and further propose a general class of information propagation model interpolating the two classic models after extensions. The proposed model has the additional feature that it can be freely reduced to either classic model by setting appropriate model parameters. A second contribution of our paper is a general framework for the IM problem, in order to enlarge the family of applicable objective functions. The framework introduces MINLP to the IM problem, where we consider derivative-free methods as general solutions and further propose the customised method with local convergence, based on the features of the proposed model.

The rest of our paper is organised as follows. In Sec. II, we discuss in detail the IC model and the LT model. In Sec. III, we propose the general class of information propagation model and illustrate its salient features. In Sec. IV, we propose the general framework for the IM problem, and the customised method. The numerical results of both the general model and the proposed method are discussed in Sec. V. Finally, we conclude with some implications for future work in Sec. VI. In Appendix, we include detailed theoretical results, and further features of the proposed model and the IM problem.

II. RELATED WORK

We first describe the two classic information propagation models, the IC model and the LT model, in more detail [10, 11]. In both models, each individual node has two state values, either 0 for being inactive or 1 for being active, and the primary focus is on progressive processes, where nodes can switch from being inactive to being active but not vice versa. Importantly, there is no feedback between nodes, even on undirected networks, as a node can not be influenced by another node that it influenced

before. Specifically, in the LT model, a node v_j is influenced by each neighbour v_i according to a weight b_{ij} s.t. $\sum_i b_{ij} \leq 1$, where $b_{ij} = 0$ if node v_i is not v_j 's neighbour; each node v_j chooses a threshold θ_j uniformly at random from the range $[0, 1]$, which represents the critical influence weight necessary for node v_j to be activated. Given a random choice of the thresholds, and an initial set of active nodes \mathcal{A}_0 , the propagation process unfolds deterministically in discrete time steps, where in step $t > 0$, all nodes that are active in step $t - 1$ remain active, and an inactive node v_j will be activated if the total weight of its active neighbours is at least its threshold θ_j , i.e.

$$\sum_{v_i \in \mathcal{A}_{t-1}} b_{ij} \geq \theta_j, \quad (1)$$

where set \mathcal{A}_{t-1} contains the active nodes in step $t - 1$. However, in the IC model, each activated node v_i has a single chance to activate each currently inactive neighbour v_j when it first becomes active, with success probability p_{ij} independently of the history thus far. If v_j is successfully activated, it will have value 1 in the next time step, but whether or not v_i succeeds, it cannot further attempt to activate its neighbours in the subsequent rounds. More general cascade and (submodular) threshold models have also been considered [7, 10]. In particular, Kempe et al. [10] considered the variants of both models with feedback through constructing a multilayer with each layer for each time step, but they required a predetermined depth of the propagation. We refer the readers to [26] for a comprehensive survey on information propagation.

The IM problem under the two classic models is NP hard, and the key algorithmic breakthrough lies in the approximation guarantees for the greedy hill-climbing algorithms [10]. Subsequently, several methods have been proposed to further improve the efficiency of the greedy algorithms, maintaining the same approximation guarantees [17, 19], or not exactly [27–29]. One vital assumption is that the information spread is *submodular*. Specifically, a function $f : P(U) \rightarrow \mathbb{R}^+ \cup \{0\}$, where $P(U)$ is the power set of a finite set U , is submodular, if

$$f(S \cup \{v\}) - f(S) \geq f(T \cup \{v\}) - f(T),$$

for all element $v \in U$ and $S \subseteq T \subseteq U$. We refer the readers to [20, 21] for more detailed description of the development of the IM problem. However, more general class of functions could occur in certain scenarios. For the LT model, the key correspondence lies in the uniform distribution of thresholds, and it is straightforward to show that the influence spreading under the LT model with deterministic thresholds is not submodular. Furthermore, with deterministic thresholds, the IM problem has been shown to be NP-hard to approximate within a factor of $n^{1-\epsilon}$ for any $\epsilon > 0$ [30, 31]. Meanwhile, fully linear models have been considered in maximising the influence, where they connect the best strategy with existing centrality measures [32], or propose new ones to

characterise the spread [33, 34]. Continuous-valued interventions have also been analysed in the IM context [35]. However in this paper, we are interested in the case when the main constraint lies in the number of initially activated nodes, and we can consider, e.g., companies have limited time and energy to convince more people to buy the products.

III. GENERAL CLASS OF INFORMATION PROPAGATION MODEL

In this section, we propose a novel class of information propagation model, with continuous state variables while allowing the feedback between states. The full description of the proposed model is in Sec. III A. We show that it can be reduced to the extended IC model in Sec. III B 1 and the extended LT model in Sec. III C 1, as well as its general properties via the corresponding differences in Sec. III B 2 and Sec. III C 2 respectively. These overall demonstrate the unique characteristics of the proposed model.

A. Model description

Consider a social network $G(V, E)$, where $V = \{v_1, v_2, \dots, v_n\}$ is the node set, and $E = \{(v_i, v_j) : \text{there is an edge from node } v_i \text{ to node } v_j\}$ is the edge set. Each edge (v_i, v_j) is considered as a channel connecting nodes v_i and v_j from which the information flows, and can be associated with a weight W_{ij} , for example, indicating the level of trust. The state value $x_i(t) \in \mathbb{R}$ describes the amount of information accepted of node v_i at each time step $t \geq 0$, and $\mathbf{x}(t) = (x_i(t))$ denotes the vector consisting of $x_i(t)$.

We construct the model as follows. Suppose that at $t > 0$, an amount $y_j(t; i)$ information is sent to node v_j from its neighbour v_i in order to influence it. We assume that this value is proportional to the accepted information of v_i at the previous step, $x_i(t-1)$. We further assume that this relation between v_j and v_i is *independent* of the following quantities: (i) $x_r(t')$, $\forall t' < t-1$, $v_r \in V$, so that only the previous states impact the present state in a Markov-like fashion, (ii) $x_j(t-1)$, so that each node freely receives information from its neighbours independently of its own state, and (iii) $x_r(t-1)$, $\forall r \neq i, j$, which aligns with the notion of independent attempts from the IC model. Moreover, the information flows from node v_i to node v_j through the edge connecting them, and we assume the edge weight W_{ij} contains all the factors that may affect, either enlarge or reduce, the transmission of information. Therefore explicitly, we assume $y_j(t; i) = W_{ij}x_i(t-1)$. However, the decision to accept the information received is based on the *collective* behaviour of the whole neighbourhood. This step is implemented by applying a non-linear transformation to $y_j(t) = \sum_i y_j(t; i)$, in order to capture how the accumu-

lated information received from all neighbours transforms into a change for the state of v_j , which is reminiscent of the mechanisms of the LT model, but also of non-linear models for opinion dynamics [36]. Specifically, we assume that at each step, there is a lower bound $l_{j,t}$ in the model, corresponding to the critical mass to trigger the propagation s.t. $x_j(t) = 0$ if $y_j(t) < l_{j,t}$, and also an upper bound $h_{j,t}$ for the saturation effect s.t. $x_j(t) = h_{j,t}$ if $y_j(t) \geq h_{j,t}$ [37, 38] (see Fig. 1 for a step-by-step illustration of the underlying process which we will discuss later). Therefore, the general class of information propagation model we propose is a bounded-linear dynamics,

$$x_j(t) = f_{j,t} \left(\sum_i W_{ij} x_i(t-1) \right), \quad \forall t > 0, v_j \in V, \quad (2)$$

$$\text{where } f_{j,t}(x) = \begin{cases} 0, & x < l_{j,t}, \\ x, & l_{j,t} \leq x < h_{j,t}, \\ h_{j,t}, & x \geq h_{j,t}, \end{cases}$$

is the time-dependent bound function of each node v_j (see Fig. 2 for an example), $\mathbf{W} = (W_{ij})$ with $W_{ij} \geq 0$ is the (weighted) adjacency matrix of the underlying network, $\{l_{j,t}\}$ and $\{h_{j,t}\}$ are the time-dependent lower and upper bounds of each node v_j , respectively, with $0 \leq l_{j,t} \leq h_{j,t}$. The initial states $\mathbf{x}(0)$ are given, with $x_j(0) \in \{0\} \cup [l_{j,0}, h_{j,0}]$ and $l_{j,0} > 0$.

In the proposed model, Eq. (2) determines the time evolution of influence at time t , and a node v_j is *influenced*, or *active*, at time t if $x_j(t) > 0$. We represent the *overall influence* on each node v_j as

$$s_j = \sum_{t=1}^{\infty} (1-\gamma)^t x_j(t), \quad (3)$$

where $\gamma \in [0, 1)$ is a time-discounting factor which guarantees convergence.

In order to interpret the model (2) and the underlying process more intuitively, we construct a small undirected social network with seven agents, as in Fig. 1, with a uniform weight $\alpha = 0.4$. For illustrative purposes, we apply the bounds $l_{j,t} = 0.8^t$ and $h_{j,t} = 2 \times 0.8^t$, $\forall t \geq 0$, $v_j \in V$, set $\gamma = 0$, and activate nodes v_1, v_2 with value 2 and node v_3 with value 1 at $t = 0$. In this configuration, nodes v_1, v_2 and v_2, v_3 can collectively influence v_4, v_5 , respectively, at $t = 1$; while at $t = 2$, v_4 can influence v_1 on its own, as a result of its high state value, while v_5 cannot influence v_7 on its own; see Fig. 1. This implies that the underlying process can have features both close to the IC model, and also towards the LT model, as in time step 2. The combination of these features is desirable since a social network can have people with heterogeneous levels of activity, where nodes of high activity are more likely to activate others. Moreover, there is a positive feedback among the nodes v_2, v_4, v_5, v_6 , as they reinforce their states in the current configuration; see Fig. 3. In real social networks, we can consider that groups of close friends keep receiving positive feedback from each other, thus reinforcing information over time.

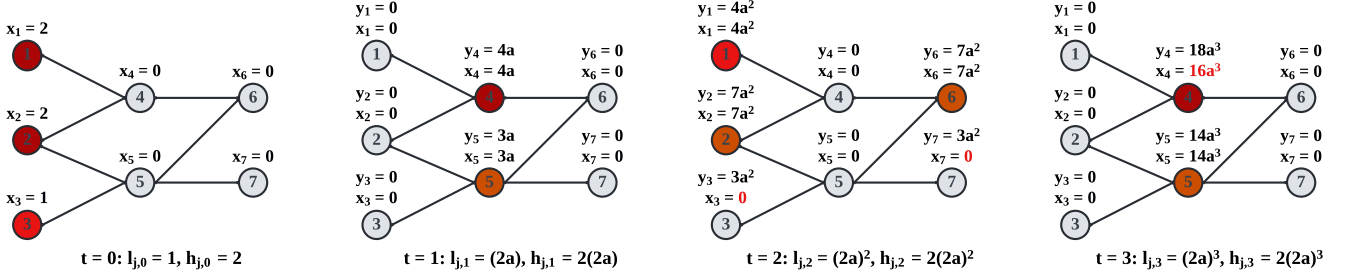


FIG. 1. Illustration of the information propagation in the first few steps following the proposed model, where $y_j(t) = \sum_i W_{ij}x_i(t-1)$ is the linear product, $x_j(t) = f_{j,t}(y_j(t))$ is the state value, the network has uniform weight α , and the bounds are set to be $l_{j,t} = (2\alpha)^t, h_{j,t} = 2(2\alpha)^t, \forall v_j \in V$, with the node color indicating the level of influence at each step.

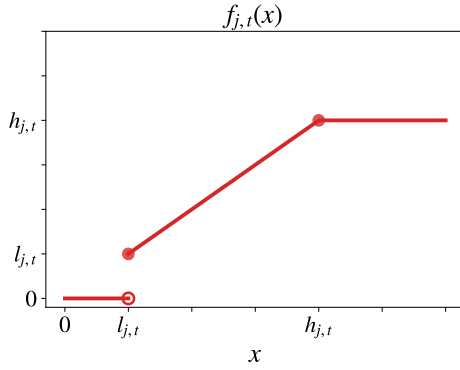


FIG. 2. Example bound function $f_{j,t}$ of node v_j at time step t where $h_{j,t} = 4l_{j,t} > 0$.

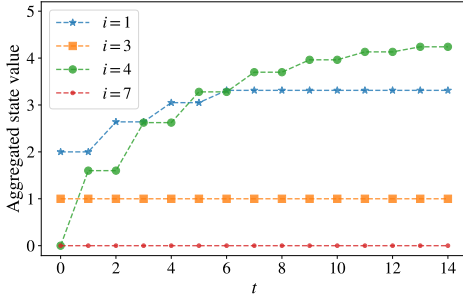


FIG. 3. The change of the sum of state values $\sum_{t'=0}^t x_j(t')$ of selected nodes along time t (bottom) on the network in Fig. 1 with uniform weight $\alpha = 0.4$.

In the following, we will elaborate on the features of the proposed model through the relation and differences with the classic models from a quantitative perspective.

B. Extreme I: The linear dynamics

When both bounds are sufficiently loose, the model reduces to the *linear dynamics* of unbounded state vari-

ables, where

$$\mathbf{x}(t) = \mathbf{W}^T \mathbf{x}(t-1), \quad \forall t > 0, \quad (4)$$

where \mathbf{W} is the (weighted) adjacency matrix of the network. Here, the following condition on the time-discounting factor γ and the spectral radius $\rho(\mathbf{W})$ is required to guarantee the convergence of the overall influence,

$$\gamma > 1 - 1/\rho(\mathbf{W}). \quad (5)$$

The linear dynamics can be considered as an extension to the classic IC model for continuous state variables in the deterministic case. In the classic *probabilistic* IC model, each edge weight W_{ij} corresponds to the probability that node v_i can influence node v_j in a Bernoulli trial, thus the expected amount of contribution to the state value of v_j from v_i in one step. Then for the expected or *deterministic* case, if we assume that (i) the expected value is the actual amount of information accepted by each node, and (ii) the state values have the *no-memory* property where the ability to either receive or send information at the current t step is independent of its previous states, we have $x_j(t) = \sum_i W_{ij}x_i(t-1), \forall v_j \in V$, i.e. the extended IC model has the same updating function as the linear dynamics in Eq. (4).

1. Relation between the models

Here, we give the detailed correspondence between the proposed model and the linear dynamics by quantifying “sufficiently loose”, while leave the detailed proof to Appendix A 1.

Lemma 1. *If $l_{j,t} \leq l_{\min,0} w^t \leq h_{j,t}, \forall t > 0, v_j \in V$, where $l_{\min,0} = \min_j l_{j,0}$ and $w = \min_{ij: W_{ij} > 0} W_{ij}$, in the proposed model (2), then there is no threshold effect from the lower bounds, i.e. $\forall t > 0, v_j \in V$ s.t. $\sum_i W_{ij}x_i(t-1) > 0$,*

$$\sum_i W_{ij}x_i(t-1) \geq l_{j,t}. \quad (6)$$

Theorem 2. If $l_{j,t} \leq l_{\min,0} w^t \leq h_{\max,0} \max_j \mathbf{1}^T \mathbf{W}_{:,j}^t \leq h_{j,t}, \forall t > 0, v_j \in V$, where $\mathbf{1}$ is the all-one vector, $\mathbf{W}_{:,j}^t$ is the j -th column of \mathbf{W}^t , $h_{\max,0} = \max_j h_{j,0}$, and $l_{\min,0}, w$ are the same as in Lemma 1, the proposed model (2) is equivalent to the linear dynamics (4).

2. Differences between the models

We now illustrate the general properties of the proposed model via deviating it from the linear dynamics. Specifically, we analyse the imposed threshold effect when increasing the lower bounds, where nodes with more overlap in their neighbourhoods of various distances will be able to achieve a higher influence on all nodes, through the lens of stochastic block models (SBMs) (see Appendix A1 for the detailed proof). In Claim 1, we consider specifically a two-block planted SBM, $SBM(p_{in}, p_{out})$, where it has two communities, and the probabilities for an edge to occur inside each community and between the two communities are p_{in} and p_{out} , respectively.

Claim 1. With $l_{j,0} = h_{j,0} = l_0, \forall v_j \in V$, and $\{h_{j,t}\}$ as in Theorem 2 in the proposed model (2), $SBM(p_{in}, p_{out})$ with two equally sized communities, $\mathcal{B}_1, \mathcal{B}_2$, and uniform weight α has the following properties at $t = 1$:

1. when $l_{j,1} \leq l_1^* = l_0 \alpha, \forall v_j \in V$, the expected influence $\mathbb{E}[\sum_j (1 - \gamma) x_j(1)]$ from the initially activated node set (i) $\mathcal{A}_0 = \{v_{i_1}, v_{i_2}\} \subset \mathcal{B}_1$, is the same as that from (ii) $\mathcal{A}_0 = \{v_{j_1}, v_{j_2} : v_{j_1} \in \mathcal{B}_1, v_{j_2} \in \mathcal{B}_2\}$;
2. when $l_1^* < l_{j,1} \leq 2l_1^*, \forall v_j \in V$ [39], if

$$p_{in} \neq p_{out}, \quad (7)$$

the expected influence $\mathbb{E}[\sum_j (1 - \gamma) x_j(1)]$ from set (i) is larger than that from set (ii).

C. Extreme II: The linear threshold model

With every upper bounds equal to the corresponding lower bounds, all the bound functions only have *threshold* effect on the *linear* product, where for each node v_j at each time step $t > 0$,

$$x_j(t) = \begin{cases} l_{j,t}, & \sum_i W_{ij} x_i(t) \geq l_{j,t}, \\ 0, & \text{otherwise,} \end{cases} \quad (8)$$

with \mathbf{W} being the (weighted) adjacency matrix of the network.

The proposed model in this case can be treated as an extension to the classic LT model for continuous variables and deterministic thresholds. Firstly, we maintain the

linear activation strategy as in (1), but instead of value 1 we plug in the corresponding state values. Secondly, with continuous variables, we can control the source of nonlinearity to be only the activation, through setting the activated state value to be the threshold value. Note that the state values can then change magnitude along time, thus we impose time-dependent thresholds $\{\theta_{j,t}\}$. Thirdly, we also assume the no-memory property as in Sec. IIIB. These jointly give the updating function (8), with $h_{j,t} = l_{j,t} = \theta_{j,t}$, and we refer to this extension as the extended LT model hereafter.

1. Relation between the models

To further disentangle the relationship between the proposed model and the threshold models, we consider the following *threshold-type* bounds, where for each node v_j at each time step $t > 0$,

$$\begin{aligned} l_{j,t} &= (\theta_{l,j} \alpha)^t l_{j,0}, \\ h_{j,t} &= \theta_{h,j} \theta_{l,j}^{t-1} \alpha^t h_{j,0}, \end{aligned} \quad (9)$$

$\alpha = \sum_{(v_i, v_j) \in E} W_{ij} / |E|$ is the mean weight, and $\theta_{l,j}, \theta_{h,j}$ are the thresholds for the upper and lower bounds, respectively, with $0 \leq \theta_{l,j} \leq \theta_{h,j}$. With such bounds, the proposed model reduces to the extended LT model if $l_{j,0} = h_{j,0}$ and $\theta_{l,j} = \theta_{h,j}, \forall v_j \in V$.

We also consider another possibly more intuitive extension to the classic LT model, where for each node v_j at each time step t , instead of a single value of 1 for being active, it can take values in a range $[1, m_j]$ and the exact state value depends on how strong the information it receives is i.e. $\sum_i W_{ij} x_i(t-1)$. Specifically, the model has the updating function,

$$x_j(t) = f_j \left(\sum_i W_{ij} x_i(t-1) \right), \quad \forall t > 0, v_j \in V, \quad (10)$$

$$\text{where, } f_j(x) = \begin{cases} 0, & x < l'_j, \\ \frac{m_j - 1}{h'_j - l'_j} (x - l'_j) + 1, & l'_j \leq x < h'_j, \\ m_j, & x \geq h'_j, \end{cases}$$

is the time-independent bound function, and $x_j(0) \in [1, h'_{j,0}]$ with $h'_{j,0}$ being the upper bound of node v_j 's initial state value. We still represent the overall influence on each node v_j as $\sum_{t=0}^{\infty} (1 - \gamma')^t x_j(t)$, where $\gamma' \in [0, 1)$ is a time-discounting factor which guarantees convergence. As we will show later, with detailed proof in Appendix A1, the proposed model with the threshold-type bounds can be equivalent to this model with specific choice of parameters.

Theorem 3. If the threshold-type bounds have uniform thresholds s.t. $\forall v_j \in V$,

$$\theta_{l,j} = \theta_l, \theta_{h,j} = \theta_h, \quad (11)$$

the proposed model (2) with such bounds and $l_{j,0} = 1, \forall v_j \in V$, is equivalent to (10) with $l'_j = \theta_l \alpha, h'_j =$

$\theta_h \alpha h_{j,0}$, $m_j = (\theta_h h_{j,0})/\theta_l$, $h'_{j,0} = h_{j,0}$, $\forall v_j \in V$, and $\gamma' = 1 - (1 - \gamma)\theta_l \alpha$, in terms of the overall influence. Specifically, if we denote the state values from the proposed model as $x_j(t)$ and those from (10) as $x'_j(t)$,

$$x_j(t) = (\theta_l \alpha)^t x'_j(t), \quad \forall t \geq 0, v_j \in V. \quad (12)$$

From Theorem 3, we can see that if the network has uniform weight α , the proposed model with the threshold-type bounds (9) satisfying (11) and $\theta_l = \theta_h$ is equivalent to the constant threshold (CT) model, where a node will be activated if it has θ_l neighbours that are active in the previous time step [20]. Hence, the bound thresholds θ_l, θ_h can play the same role as the threshold in the CT model. Specifically, $\theta_l = \theta_h = 1$ corresponds to simple contagions, where a node can be influenced by a single active neighbour, and $\theta_l = \theta_h > 1$ corresponds to complex contagions, where collective effort from the neighbourhood is required to influence a node. For general cases of weighted networks, the bound thresholds together with the mean weight α serve the same role as the threshold in the classic LT model in (1), i.e. on the weighted sum of influenced neighbours. Due to such correspondence, we will consider exclusively the threshold-type bounds hereafter.

2. Differences between the models

We now examine the general properties of the proposed model via deviating it from the extended LT model. Particularly, we consider the locally linear effect when increasing the upper bounds through θ_h in (11) for the threshold-type bounds (9), where a single active node can influence its neighbours, while it can scarcely occur when $\theta_h = \theta_l > 1$ (see Appendix A 1 for the detailed proof).

Claim 2. *With $l_{j,0} = h_{j,0} = l_0$, $\forall v_j \in V$, and the threshold-type bounds (9) satisfying (11) applied in the proposed model (2), suppose at a particular time $t' \geq 0$, there is a tree-like structure of the active nodes at t' $\mathcal{A}_{t'} = \{v_i : x_i(t') > 0\}$ and some currently inactive node v_{j_*} s.t.*

$$\exists! v_{j_0} \in \mathcal{A}_{t'} \text{ s.t. } W_{j_0 j_*} > 0,$$

where \mathbf{W} is the (weighted) adjacency matrix. Then if the network has uniform weight α ,

1. when $\theta_h = \theta_l > 1$, node v_{j_*} can never have positive state value at $t = t' + 1$;
2. when $\theta_h > \theta_l > 1$, node v_{j_*} can have positive state value at $t = t' + 1$ given a sufficiently large θ_h .

We can take the two-block planted SBM for example again as in Sec. III B 2, and consider the case when

increasing θ_h from 2 to 4 while maintaining $\theta_l = 2$. Accordingly, we analyse the performance of the following two sets of four initially activated nodes: (i) $\mathcal{A}_0 = \{v_{i_1}, v_{i_2}, v_{i_3}, v_{i_4}\} \subset \mathcal{B}_1$; (ii) $\mathcal{A}_0 = \{v_{j_1}, v_{j_2}, v_{j_3}, v_{j_4} : v_{j_1}, v_{j_2} \in \mathcal{B}_1, v_{j_3}, v_{j_4} \in \mathcal{B}_2\}$. We show that the increase in the expected influence from (i) is more than that from (ii) in Appendix D, which is numerically verified in Sec. V A. This is because in the propagation from (i), nodes in \mathcal{B}_1 have a higher probability to reach a higher or the highest state value, thus they have a higher chance to influence their neighbours. This can be interpreted as the fact that people with high activity are more likely to influence their friends in social networks.

IV. INFLUENCE MAXIMISATION

Now, we proceed to a key algorithmic problem associated with information propagation, the *influence maximisation* (IM) problem, i.e. to maximise the overall influence on the nodes at the end of the process, and here we are interested in the constraint of a limited number of initially activated nodes, determined by the *budget size*, corresponding to the limited resource, e.g. time and energy to influence more people as discussed in Sec. II. In this section, we will first introduce a new formulation of the IM problem in Sec. IV A, and give general solutions to this task in Sec. IV B. In these two sections, we focus on the general features that the IM problem could have in practice. Then we turn to the special cases when the dynamics are given by the proposed model in Sec. IV C, and further propose a customised algorithm in Sec. IV D.

A. Problem formulation

With a given information propagation process, and a given function $s_j(\cdot)$ for the overall influence on each node v_j , the overall influence on the whole network is naturally,

$$s(\mathbf{x}(0)) = \sum_j s_j(\mathbf{x}(0)), \quad (13)$$

where $\mathbf{x}(0)$ is the initial state vector. The IM problem is then to maximise $s(\mathbf{x}(0))$ with respect to the $\mathbf{x}(0)$, subject to the constraint of limited budget size,

$$|\{v_j : x_j(0) > 0\}| \leq k, \quad (14)$$

where $k \in \mathbb{Z}^+$ is the budget size.

We then formulate the IM problem with objective (13) and constraint (14) as a *mixed-integer (nonlinear) pro-*

gramming (MINLP),

$$\begin{aligned}
& \max_{\mathbf{x}, \mathbf{z}} && s(\mathbf{x}) \\
& \text{s.t.} && x_j \leq h_{j,0} z_j, \\
& && x_j \geq l_{j,0} z_j, \\
& && \sum_j z_j \leq k, \\
& && x_j \in \mathbb{R}, z_j \in \{0, 1\}, \forall j,
\end{aligned} \tag{15}$$

where $0 < l_{j,0} \leq h_{j,0}$ restrict the initial level of influence of node v_j , $k \in \mathbb{Z}^+$ is the budget size, and the objective function $s(\cdot)$ is the overall influence on the whole network as in Eq. (13). The variables in vector \mathbf{x} correspond to the initial states, while the variables in vector \mathbf{z} , of the same dimension, are added to appropriately impose the constraint (14).

The difficulty of the optimisation problem lies in the objective function $s(\mathbf{x})$. Take the proposed model for example. (i) $s(\mathbf{x})$ is not always smooth and even discontinuous, since each $f_{j,t}(x)$ in (2) can be nonsmooth at $h_{j,t}$ and discontinuous at $l_{j,t}$. (ii) A closed-form of $s(\mathbf{x})$ cannot be obtained generally, except when $f_{j,t}(x) = x$, $\forall t > 0$, $v_j \in V$, in (2). (iii) The derivative information is rarely very useful in finding a maximal point, as discussed in Appendix B 3. However, even for the proposed model with the influence function in Eq. (3), we can show that the evaluation of the objective function can be solved in $O(|E|t_\epsilon)$ time, where $|E|$ is the number of edges and t_ϵ is the number of time steps required for convergence of the underlying information propagation process with tolerance ϵ , as in Theorem 4. This is a bonus in the deterministic setting [40]. Hence, it is necessary to treat the objective function as an input-output (black-box) system and resort to derivative-free methods (DFMs) which we will discuss in the following section.

Theorem 4. *Given a network $G(V, E)$ with the weight matrix \mathbf{W} and an initial state $\mathbf{x}(0)$, the problem of exactly computing the function $s(\mathbf{x}(0))$ in (13) with the information propagation process (2) and the influence function (3) can be solved in $O(|E|t_\epsilon)$ time, where t_ϵ is the number of time steps required for the convergence of the underlying process with tolerance $\epsilon > 0$.*

Proof. The time complexity follows from Alg. 1. In each iteration t , each nonzero element of the weight matrix \mathbf{W} has only one chance to be used to potentially adjust the state value $\mathbf{x}^{(t)}$, and there are overall $O(|E|)$ such elements. Therefore, the time complexity of each iteration is $O(|E|)$, and the overall evaluation has time complexity $O(|E|t_\epsilon)$, dependent on the number of steps towards convergence, t_ϵ . \square

Algorithm 1 Influence evaluation.

```

1: Input: A network  $G(V, E)$  with its weight matrix  $\mathbf{W}$ 
   where  $W_{ij} > 0$  if  $(v_i, v_j) \in E$ , parameters  $\{l_{j,t}\}$ ,  $\{h_{j,t}\}$  in
   the information propagation process (2), the initial state
    $\mathbf{x}(0)$  where  $x_j(0) \in [l_{j,0}, h_{j,0}]$  if and only if  $v_j \in \mathcal{A}_0$  (0
   otherwise), and the tolerance  $\epsilon$ .
2: Output: The objective value  $s$  as in (13).
3: Set  $t \leftarrow 0$ ,  $\mathbf{x}^{(0)} \leftarrow \mathbf{x}(0)$ , and  $s \leftarrow 0$ .
4: Mark all the out-neighbours of  $\mathcal{A}_0$  as potentially activated
   nodes,  $\mathcal{N}_0 \leftarrow \bigcup_{v_j \in \mathcal{A}_0} \mathcal{N}^{out}(v_j)$ .
5: while  $|\mathbf{x}^{(t)}| > \epsilon$  do
6:    $\mathcal{A}_{t+1}, \mathcal{N}_{t+1} \leftarrow \emptyset$ , and  $\mathbf{x}^{(t+1)} \leftarrow \mathbf{0}$ ;
7:   for each potentially activated node  $v_j \in \mathcal{N}_t$  do
8:      $x_j^{(t+1)} = f_{j,t}(\sum_{i \in \mathcal{A}_t} W_{ij} x_i^{(t)})$ ;
9:     if  $x_j^{(t+1)} > 0$  then
10:       $\mathcal{A}_{t+1} \leftarrow \mathcal{A}_{t+1} \cup \{v_j\}$ ;
11:       $\mathcal{N}_{t+1} \leftarrow \mathcal{N}_{t+1} \cup \mathcal{N}^{out}(v_j)$ ;
12:       $s \leftarrow s + x_j^{(t+1)}$ ;
13:     end if
14:   end for
15:    $t \leftarrow t + 1$ ;
16: end while

```

B. General solutions

Since we cannot assume the objective to fall in a simple family, e.g. polynomials, *model-based* methods are not appropriate in this problem. This effectively limits the choice among algorithm classes for its solution to that of *direct-search* methods. Among such algorithms, the mesh adaptive direct search (MADS) method is the only one that has local convergence analysis when the objective function is not necessarily Lipschitz continuous [41]. Therefore, we consider the MADS for mixed variables (MV) [25] as a general solution to the IM problem, which can be implemented by the software NOMAD [42, 43].

Here, we introduce the important notion of *local optimality* for mixed variables, and accordingly, the *local neighbourhood*. We partition each vector into its continuous and discrete components, $\mathbf{y} = (\mathbf{y}^c, \mathbf{y}^d) \in \Omega$, where Ω is the domain. For the continuous variables of maximum dimension n^c , the neighbourhood is well-defined as the open ball, $B_\epsilon(\mathbf{y}^c) = \{\mathbf{y}' \in \mathbb{R}^{n^c} : \|\mathbf{y}' - \mathbf{y}^c\| < \epsilon\}$ with $\epsilon > 0$. However, different notions of the discrete neighbourhood exist. One common choice for integer variables is $\mathcal{N}(\mathbf{y}) = \{\mathbf{y}' \in \Omega : \mathbf{y}'^c = \mathbf{y}^c, \|\mathbf{y}'^d - \mathbf{y}^d\|_1 \leq 1\}$. With a user-defined discrete neighbourhood, the classical definition of local optimality can be extended to mixed variable domains as follows.

Definition 1. *A point $\mathbf{y} = (\mathbf{y}^c; \mathbf{y}^d) \in \Omega$ is said to be a local maximiser of a function f on Ω with respect to the set of neighbours $\mathcal{N}(\mathbf{y}) \subset \Omega$ if there exists an $\epsilon > 0$ such*

that $f(\mathbf{y}) \geq f(\tilde{\mathbf{y}})$ for all $\tilde{\mathbf{y}}$ in the set

$$\Omega \cap \left(\bigcup_{\mathbf{y}' \in \mathcal{N}(\mathbf{y})} B_\epsilon(\mathbf{y}'^c) \times \mathbf{y}'^d \right),$$

where $B_\epsilon(\mathbf{y}^c) = \{\mathbf{y}' \in \mathbb{R}^{n^c} : \|\mathbf{y}' - \mathbf{y}^c\| < \epsilon\}$ with $\epsilon > 0$ is an open ball, and $\mathcal{N}(\mathbf{y})$ is a user-defined discrete neighbourhood.

As mentioned before, MADS is among the few algorithms that can relax the assumptions for convergence analysis to include discontinuous functions. To conclude the analysis, we mention that there are many heuristic algorithms in derivative-free methods [44], but without any convergence guarantee, and refer the readers to the work of Boukouvala et al. [23] for a thorough review of DFMs in conjunction with MINLP problems.

C. Special cases

In the previous sections, we have analysed the highly general features of the IM problem, and given general solutions accordingly. Hereafter, we turn our attention to two special cases of the problem following the proposed information propagation model (2) and the influence function (3), in order to shed light on other more general cases.

The first special case is when the lower bounds, $\{l_{j,t}\}$, are sufficiently small, where we can show that the objective function $s(\cdot)$ is continuous and concave with respect to the continuous variables \mathbf{x} as in Theorem 5 (see Appendix A 2 for the detailed proof). Then any local maximum is a global maximum, therefore the direct search algorithms can have global convergence, though it is only with respect to the continuous variables since the optimality of the integer part is still local, from Definition 1.

Theorem 5. *If $\{l_{j,t}\}, \{h_{j,t}\}$ are as in Lemma 1, then the objective function $s(\cdot)$ in the IM problem (15) is continuous and concave w.r.t. the continuous variables \mathbf{x} .*

Furthermore, we can also show that the objective is Lipschitz continuous by noting that $0 \leq f_{j,t}(x) \leq x$, $\forall t > 0, v_j \in V$ and potential value x . In this case, there are methods proven to have global convergence, for example the new derivative-free line-search type algorithms [45]. Meanwhile, the condition of the lower bounds could be looser in practice, since, for example, the propagation does not necessarily go through the edge(s) of the smallest weight in every step. Therefore, we can have a larger region of the parameters where the objective function is (Lipschitz) continuous and concave.

The other special case is when not only $\{l_{j,t}\}$ are sufficiently small but $\{h_{j,t}\}$ are sufficiently large, i.e. the linear-dynamics extreme as in Sec. III B. Hence,

$$\mathbf{x}(t) = \mathbf{W}^T \mathbf{x}(t-1) = (\mathbf{W}^T)^t \mathbf{x}(0),$$

and the objective function is then,

$$\begin{aligned} s(\mathbf{x}(0)) &= \sum_j \sum_{t=1}^{\infty} (1-\gamma)^t x_j(t) \\ &= \sum_{t=1}^{\infty} \mathbf{1}^T ((1-\gamma)\mathbf{W}^T)^t \mathbf{x}(0) \\ &= \mathbf{1}^T \left((\mathbf{I} - (1-\gamma)\mathbf{W}^T)^{-1} - \mathbf{I} \right) \mathbf{x}(0) = \mathbf{c}^T \mathbf{x}(0), \end{aligned} \quad (16)$$

where $\mathbf{c} = ((\mathbf{I} - (1-\gamma)\mathbf{W})^{-1} - \mathbf{I})\mathbf{1}$ is the Katz centrality with factor $(1-\gamma)$, \mathbf{I} is the identity matrix, and the penultimate equation is obtained given that condition (5) is true in the linear-dynamics extreme. Hence, the objective function is linear, thus (Lipschitz) continuous, concave and smooth. The exact solution in this case is achievable as in Theorem 6, and we defer the detailed proof to Appendix A 2.

Theorem 6. *When $\{l_{j,t}\}, \{h_{j,t}\}$ are as in Theorem 2, then the exact solution to the IM problem (15) is*

$$x_j^* = \begin{cases} h_{j,0}, & \text{if } j \in \mathcal{A}, \\ 0, & \text{otherwise,} \end{cases} \quad z_j^* = \begin{cases} 1, & \text{if } j \in \mathcal{A}, \\ 0, & \text{otherwise,} \end{cases} \quad (17)$$

where $\mathcal{A} = \{j_1, \dots, j_k\}$ s.t. $h_{i,0}c_i \leq h_{j,0}c_j$, $\forall i \notin \mathcal{A}, j \in \mathcal{A}$, and $\mathbf{c} = ((\mathbf{I} - (1-\gamma)\mathbf{W})^{-1} - \mathbf{I})\mathbf{1}$ is the Katz centrality with factor $(1-\gamma)$.

Hence, the exact solution when the proposed model is in the linear-dynamics extreme is to activate the k nodes of the highest product of its Katz centrality and its maximum initial value. This relates the IM problem to a well-studied centrality measure in networks, the Katz centrality. Furthermore, this solution can serve as a warm start in the following search algorithm for the IM problem in a general case, with the search depth potentially proportional to the distance of the underlying propagation from the linear dynamics.

D. Customised direct search

Here, we exploit one feature of the objective, that $s(\mathbf{x})$ is non-decreasing in \mathbf{x} , which is inherited in the proof of Theorem 6, and accordingly propose a customised direct search method for the IM problem.

To see why $s(\mathbf{x}(0))$ is non-decreasing in $\mathbf{x}(0)$, we first show that $\mathbf{x}(t)$ is non-decreasing in $\mathbf{x}(0)$, $\forall t > 0$. This can be proven by induction: (i) $\mathbf{x}(1)$ is non-decreasing in $\mathbf{x}(0)$, since each $f_{j,1}(\cdot)$ and each linear function $h_j(\mathbf{x}) = \sum_i W_{ij}x_i$ in (2) are non-decreasing; (ii) suppose $\mathbf{x}(t)$ is non-decreasing in $\mathbf{x}(0)$, $\forall t \leq t'$, then we can show that $\mathbf{x}(t'+1)$ is non-decreasing in $\mathbf{x}(0)$, since $\mathbf{x}(t'+1)$ is non-decreasing in $\mathbf{x}(t')$ by the same logic as (i) and $\mathbf{x}(t')$ is non-decreasing in $\mathbf{x}(0)$ by the induction hypothesis. Hence, $s(\mathbf{x}(0)) = \sum_j \sum_{t=0}^{\infty} (1-\gamma)^t x_j(t)$ is non-decreasing in $\mathbf{x}(0)$.

Accordingly, to maximise the objective $s(\mathbf{x})$ with respect to \mathbf{x} and \mathbf{z} in the MINLP (15), is equivalent to the maximisation with \mathbf{x} thus \mathbf{z} at their highest possible values, particularly $x_j = h_{j,0}z_j$ and $\sum_j z_j = k$, i.e.

$$\begin{aligned} \max_{\mathbf{z}} \quad & s(\mathbf{h}_0 \odot \mathbf{z}) \\ \text{s.t.} \quad & \sum_j z_j = k, \\ & z_j \in \{0, 1\}, \forall j, \end{aligned} \quad (18)$$

where $\mathbf{h}_0 = (h_{j,0})$, and \odot denotes the element-wise (Hadamard) product. Then the domain Ω^d is a natural mesh to search at each iteration r ,

$$M_r = \Omega^d = \{\mathbf{z} \in \{0, 1\}^n : \sum_j z_j = k\}. \quad (19)$$

The constraints are incorporated in the domain, and are treated by the extreme barrier approach s_{Ω^d} , where $s_{\Omega^d}(\mathbf{z}) = s(\mathbf{h}_0 \odot \mathbf{z})$ if $\mathbf{z} \in \Omega^d$ and $-\infty$ otherwise. We define the neighbourhood function of binary variables \mathbf{z} to be,

$$\mathcal{N}(\mathbf{z}) = \{\mathbf{y} \in \{0, 1\}^n : \|\mathbf{y} - \mathbf{z}\|_1 \leq d\}, \quad (20)$$

where $d \in \mathbb{Z}^+ \setminus \{1\}$, since $\|\mathbf{z}' - \mathbf{z}\|_1 \geq 2$ if $\mathbf{z}' \neq \mathbf{z}$ and $\mathbf{z}', \mathbf{z} \in \Omega^d$, where the shortest distance of 2 occurs when exchanging only one element of value 1 with another of value 0.

We then propose the following *customised direct search* (CDS) algorithm for the revised MINLP (18). In this algorithm, we search the local neighbourhood of the current candidate $\mathbf{z}^{(r)}$ at each iteration r in the `poll` step, until a point with sufficient improvement in the objective value has been found or all points have been exhausted. In the termination check, if an improved point has been found, the algorithm will go back to the optional `search` step, but will decrease the required improvement if a sufficiently improved point has not been found, while, if no improvement has been found, the algorithm terminates; see Alg. 2 for more details. The default parameter values are set to be $\zeta = 0.1$, $\delta = 0.5$ and $d = 2$.

Algorithm 2 Customised direct search (CDS).

- 1: **Initialisation**: Set $0 < \zeta, \delta < 1$. Let $\mathbf{z}^{(0)} \in \Omega^d$ such that $z_j^{(0)} = 1$ if node $j \in \mathcal{A} = \{j_1, \dots, j_k\}$ where $h_{i,0}c_i \leq h_{j,0}c_j$, $\forall i \notin \mathcal{A}, j \in \mathcal{A}$, and $\mathbf{c} = (\mathbf{I} - (1 - \gamma)\mathbf{W})^{-1}\mathbf{1}$ is the Katz centrality. Set iteration $r = 0$.
 - 2: **SEARCH** step (optional): Evaluate s_{Ω^d} on a finite subset of trial points on the mesh M_r (19), until a sufficiently improved mesh point \mathbf{z} is found, where $s_{\Omega^d}(\mathbf{z}) > (1 + \zeta)s_{\Omega^d}(\mathbf{z}^{(r)})$, or all points have been exhausted. If an improved point is found, then the **SEARCH** step may terminate, skip the next **POLL** step and go directly to step 4.
 - 3: **POLL** step: Evaluate s_{Ω^d} on the set $\Omega^d \cap \mathcal{N}(\mathbf{z}^{(r)}) \subset M_r$ as in (20), until a sufficiently improved mesh point \mathbf{z} is found, where $s_{\Omega^d}(\mathbf{z}) > (1 + \zeta)s_{\Omega^d}(\mathbf{z}^{(r)})$, or all points have been exhausted.
 - 4: **Termination check**: If an improvement is found, set $\mathbf{z}^{(r+1)}$ as the improved solution, while decreasing $\zeta \leftarrow \delta\zeta$ if a sufficient improvement has not been found, increment $r \leftarrow r + 1$, and go to step 2. Otherwise, output the solution $\mathbf{z}^{(r)}$.
-

Therefore, local convergence is directly guaranteed in the termination step, by Definition 1. Global convergence could possibly be obtained with a sophisticatedly developed `search` step and a better understanding of the landscape of the objective function, in order not to be trapped in bad local optima. However, the downside of a global method is its time complexity, thus we leave the `search` step optional. Instead, the CDS method incorporates the problem's features and circumventing the worst-case complexity by initialising with the exact solution to the linear-dynamics extreme, and we postulate that the local optima near this special solution are sufficiently good. We leave the detailed discussion of the time complexity to Appendix C 4.

From the current CDS method, there are two dimensions to further improve the quality of the output. We first note that the current problem is only of binary variables, thus is purely combinatorial, i.e. the problem is to select a set of nodes to give value 1. Accordingly, there are two known methods of global convergence: (i) *brute-force*, where all node sets of size k are evaluated in order to choose an optimal one; (ii) *random sampling*, where randomly chosen node sets are evaluated, and this method has global convergence asymptotically if it samples densely enough. The two dimensions of improvement are motivated by these two methods. On the one hand, we can enlarge the distance in defining the neighbourhood, which necessarily searches more points in the domain. Further, if the neighbourhood is as large as the whole domain, it reduces to the brute-force method. On the other hand, we can restart the searching process, i.e. steps 2,3,4 in Alg. 2, from other unexplored points randomly, which works in the same logic as the `search` step. This strategy will give global convergence asymptotically, similar to the random sampling method.

V. NUMERICAL EXPERIMENTS

In this section, we experimentally illustrate the rich behaviour of the general class of information propagation model, and evaluate the performance of the CDS method for the IM problem in both small and large, both synthetic and real networks. Throughout the section, $l_{j,0} = h_{j,0} = 1, \forall v_j \in V, \gamma = 0$, and we apply exclusively the threshold-type bounds in (9) with condition (11), thus the upper and lower bounds vary according to the upper and lower bound thresholds, θ_h and θ_l , respectively.

A. The information propagation model

We start from the general features of the proposed model. In accordance with Sec. III, we show that the proposed model can have both the threshold effect and the locally linear effect via tuning lower and upper bounds, respectively. Such effects cannot happen simultaneously in either the linear dynamics or the (extended) linear threshold model, but may co-exist in real systems.

Specifically, we consider simple networks generated from the two-block planted $SBM(0.9, 0.1)$, where an edge is placed between the nodes in the same community with probability $p_{in} = 0.9$ and in the different communities with $p_{out} = 0.1$. We choose these values to construct networks of assortative communities, and also to have a large difference between node sets in the same community and those not, for visualising purposes [46]. The networks have size $n = 50$ and $n_c = 2$ communities, where we label the nodes in communities one and two as 0 to 24 and 25 to 49, respectively; see Fig. 4 for one realisation. We assign a uniform weight $\alpha = 0.1$, to account for general loss of information during transmission. Therefore, $\theta_l = 1$ corresponds to the critical lower bounds for the linear-dynamics extreme, where any $\theta_l > 1$ cannot always result in linear dynamics. The difference in the propagation behaviour will be quantified by the *propagation profile*, defined as the sum of (weighted) state values up to time step t on all nodes,

$$s(t) = \sum_j \sum_{t'=0}^t (1 - \gamma)^{t'} x_j(t'), \quad (21)$$

changing along t , where $\mathbf{x}(t') = (x_j(t'))$ is the state vector at time step t' with the updating function (2) and a given initial state vector $\mathbf{x}(0) = (x_j(0))$. Note that $s(t) - \sum_j x_j(0)$ is part of the objective (13) in the IM problem.

We first show the threshold effect imposed on top of the linear dynamics through tuning the lower bounds to gradually deviate from the linear-dynamics extreme, as in Sec. III B 2. Specifically, following Claim 1, we consider the following two initially activated node sets: (i) $\{0, 1\}$ from the same community; (ii) $\{0, 25\}$ from the different communities. The results numerically verify such

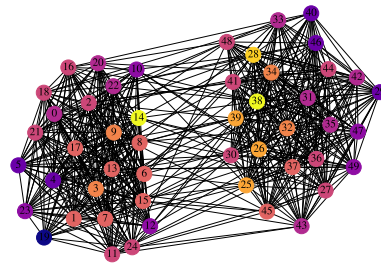


FIG. 4. One realisation of the two-block $SBM(0.9, 0.1)$.

effect, since the propagation profiles of the two sets are similar when $\theta_l = 1$, while set (i) triggers a higher value in the overall influence as θ_l slightly increases; see Fig. 5. We note that the performance of set (ii) has larger variance, and this is because it largely depends on the inter-community edges whose existence has much smaller probability. Here, the propagation profiles from set (ii) are concentrated at the values slightly above the mean (not as high as set (i)), while it also contains values substantially lower than the mean.

We then illustrate the locally linear effect added on top of the extended LT model through tuning the upper bounds to differentiate from the linear-threshold extreme. Here, we fix $\theta_l = 2$, the smallest integer for the threshold effect to take place, while increasing θ_h from 2 to a higher value, as in Sec. III C 2. We then consider the following two larger initially activated node sets: (i) $\{0, 1, 2, 3\}$ from the same community; (ii) $\{0, 1, 25, 26\}$ evenly distributed in the two communities. The numerical results justify such effect, because the propagation profile from set (i) has larger increase than the other when improving the upper bound threshold θ_h ; see Fig. 6. We also observe that the propagation triggered by set (ii) is consistently higher than the other.

Finally, we integrate the two aspects and provide a whole picture of the general features of the propose model via changing the upper and lower bounds simultaneously. Here, we consider both node-set pairs, $\{0, 1\}$ versus $\{0, 25\}$ and $\{0, 1, 2, 3\}$ versus $\{0, 1, 25, 26\}$, and quantify the change of behaviour through the *ratio* of the overall influence following the proposed model,

$$\delta(\mathcal{A}_0^{(1)}, \mathcal{A}_0^{(2)}) = s(\mathbf{x}^{(1)}(0))/s(\mathbf{x}^{(2)}(0)),$$

where $\mathbf{x}^{(1)}(0), \mathbf{x}^{(2)}(0)$ are the initial state vectors by initially activating nodes in node sets $\mathcal{A}_0^{(1)}$ and $\mathcal{A}_0^{(2)}$ respectively, and $s(\mathbf{x}(0))$ is the overall influence as in (13) with influence function (3). We observe consistent patterns of the previously analysed features: (i) the node sets in the same community have consistently higher influence as θ_l exceeds the critical value for the other set, 1 for $\{0, 25\}$ and 2 for $\{0, 1, 25, 26\}$ (which are equal to the numbers of nodes distributed in each community); (ii) the node sets in each pair generally have increasingly closer overall influence as θ_h increases; see Fig. 7. We also notice that there is a regime where increasing the upper bounds

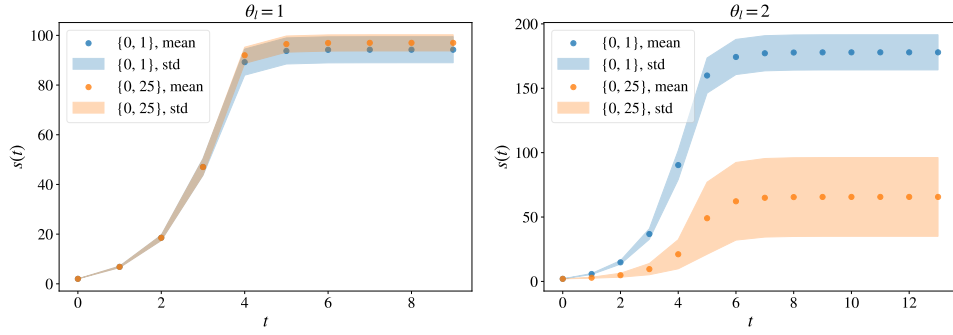


FIG. 5. The influence up to increasing time steps (x-axis), from two different initially activated node sets, with $\theta_l = 1$ (left, the critical value for the linear-dynamics extreme) and $\theta_l = 2$ (right, a larger value) while θ_h being large (here 9000), on 1000 samples of $SBM(0.9, 0.1)$.

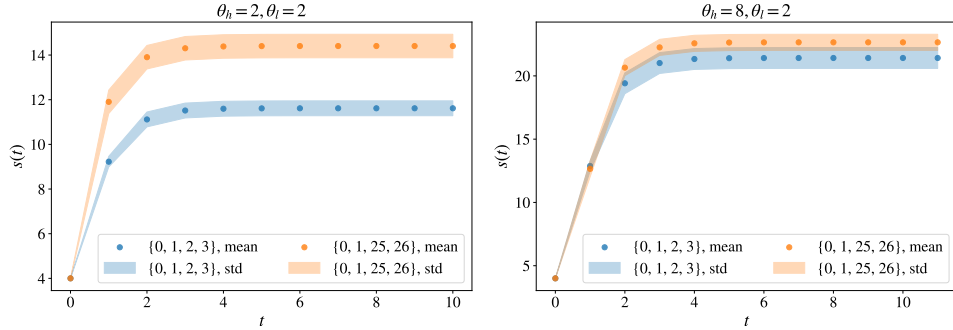


FIG. 6. The influence up to increasing time steps (x-axis), from two different initially activated node sets, with $\theta_l = 2$ while $\theta_h = 2$ (left, the linear-threshold extreme) and $\theta_h = 8$ (right, a larger value), on 1000 samples of $SBM(0.9, 0.1)$.

will enlarge the (relative) difference between the two sets, which emphasises the nonlinearity in the model.

B. Influence maximisation

We now proceed to the proposed CDS method for the influence maximisation. In the following, we first test the accuracy of the CDS method on networks on a relatively small scale. We then examine its performance on relatively large networks, both real and synthetic, by comparison with other state-of-the-art approaches.

1. The CDS method

From Sec. IVD, we know that the CDS method is a local algorithm, thus it is important to explore how good the output is with respect to the global optimum. However, algorithms with global convergence, such as the brute-force method, require $O(n^k)$ evaluations of the objective, which prohibits their application to large networks. Hence, we exclusively consider networks in a relatively small scale in this section.

In order to measure the *goodness* of the output, we consider the following two measures: accuracy and rank.

The *accuracy* is defined as the relative value to the global optimum,

$$\tau(s; s^*) = s/s^*,$$

where s is an output from the proposed algorithm, and s^* is the global optimum. $\tau(\cdot) \in [0, 1]$ and a higher accuracy implies a better solution. Since the current problem is purely combinatorial in terms of the initially activated node set, we also consider the output's *rank*,

$$\phi(\mathcal{A}_0; V, k) = \frac{|\{\mathcal{A} \subset V : |\mathcal{A}| = k, s(\mathbf{h}_0 \odot \mathbf{z}_{\mathcal{A}}) > s(\mathbf{h}_0 \odot \mathbf{z}_{\mathcal{A}_0})\}| + 1}{|\{\mathcal{A} \subset V : |\mathcal{A}| = k\}|},$$

where $G(V, E)$ is the underlying network, k is the budget size, \mathcal{A}_0 is the set of initially activated nodes corresponding to the output, $\mathbf{z}_{\mathcal{A}}$ is the binary vector whose j th element is 1 if and only if $v_j \in \mathcal{A}$, and $s(\mathbf{h}_0 \odot \mathbf{z})$ is the objective function of the revised MINLP (18). $\phi(\cdot) \in (0, 1]$, and a lower rank implies a better solution. Hence, in order to obtain the parameters in the measures, we select *brute-force* as the reference global algorithm.

Specifically, we consider the two occasions: (i) differentiating θ_l and θ_h while maintaining k , and (ii) varying k while fixing θ_l and θ_h . As a representative example, we show results exclusively from two-block SBMs, and defer

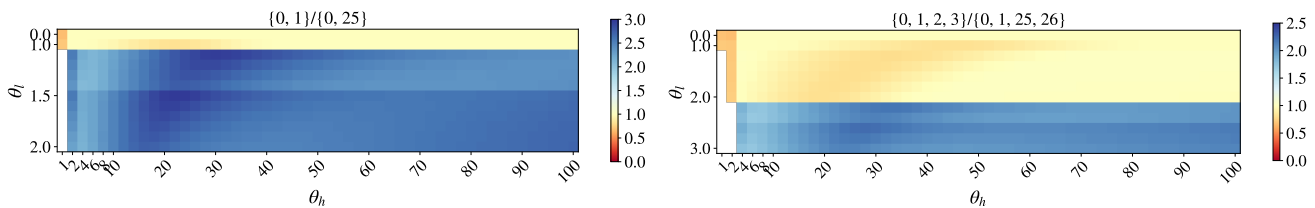


FIG. 7. The ratios of the overall influence δ from two pairs of initially activated node sets, $\{0, 1\}$ to $\{0, 25\}$ (left) and $\{0, 1, 2, 3\}$ to $\{0, 1, 25, 26\}$ (right), with changing upper bound (x-axis) and lower bound (y-axis) thresholds, on 1000 samples of $SBM(0.9, 0.1)$.

the results from other types of networks to Appendix C 3. The SBM considered here has the same size and weights as in Sec. V A, but different probabilities in the two communities, $p_1 = 0.3$ in one and $p_2 = 0.12$ in the other, in order to distinguish nodes in different communities. The connecting probability between the communities is set to be a smaller value $p_{12} = 0.01$.

When $k = 4$, the CDS method can find a solution either globally optimal or fairly close to optimal with all different combinations of the upper and lower bound thresholds; see Fig. 8. There are only 5 cases when the CDS method cannot find a globally optimal solution. However, in such worst-case scenarios, the solutions still have accuracy over 0.95 and rank less than 0.001% in overall 230,300 possibly initially activated sets, i.e. the CDS method can still output a top 2 set. Since different combinations of upper and lower bounds correspond to various properties of the underlying propagation process as discussed in Sec. III, these demonstrate that the proposed method can capture the general properties of the IM problem.

We further explore the performance of the CDS method when increasing the budget size k and $\theta_l = 2, \theta_h = 2$, one of the pairs with worst-case performance. We observe that the outputs from the CDS method generally have high accuracy (greater than 0.9), and consistently low rank; see Fig. 9. There is a drop in accuracy when k becomes larger. Apart from the drop in performance of the initial point, it is also partially because the fixed neighbourhood size, i.e. 2 here, becomes increasingly restrictive. The former is because the current dynamics are far from the linear dynamics. The latter is inherited in the CDS method being local, since one needs to define the radius of local neighbourhood. As discussed in Sec. IV D, there are two dimensions to further improve the algorithm: (i) to enlarge the radius of neighbourhood as k increases, e.g. an *adaptive* neighbourhood; (ii) to *restart* the search from some other points, preferably far from the original start. See Appendix C 3 for the strategy we propose to improve the performance.

2. Comparison between methods

In the following, we examine the performance of the CDS method on both synthetic and real networks on a relatively large scale, where we compare them with the state-of-the-art methods. Hereafter, we denote the set of initially activated nodes, \mathcal{A}_0 , as the *seed set*. We note that the vast majority of greedy algorithms following the work of Kempe et al [10] are not applicable here, because every node sets of size less than θ_l will return an overall influence 0 and then these algorithms lack an appropriate approach to select the first few nodes, which has significant consequences in their following steps. We instead compare the proposed method with the following ones.

- (i) **Random sampling** (“Random”). Randomly selecting k nodes of the network, and return them as the seed set. We repeat the process n_s times, and output the one with the highest objective value.
- (ii) **Degree-centrality method** (“Degree”). Centrality is an important measure which quantifies the significance of nodes in networks [20]. The degree-centrality method is to select the k nodes of the highest degree in the network as the seed set.
- (iii) **Katz-centrality method** (“Katz”). Finding the k nodes of the highest Katz centrality in the network as the seed set.

Since method (i) has random components, we will repeat the methods n_r times and analyse their averaged performance. In this section, we compare the performance of different methods directly through the overall influence value s .

The networks under consideration are composed of a large two-block SBM, and a real collaboration network. On the one hand, SBMs are considered here because community structure is a common feature in real networks, and also to extend the previous analysis in Sec. VB 1 to a larger scale. Collaboration networks, on the other hand, are extensively used in IM experiments, because researchers believe that such networks capture key features of social networks [47]. The specific one we select also has ground-truth communities as metadata. In the experiments, we choose $n_s = 100$ and $n_r = 10$.

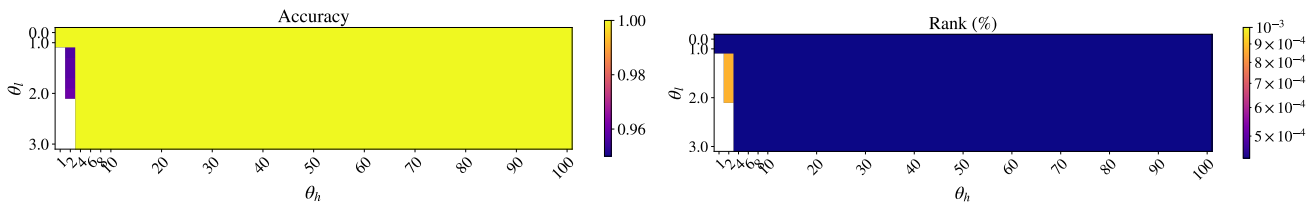


FIG. 8. Performance of the CDS method on the SBM in terms of the output’s accuracy (left) and rank (right), subject to changing upper (x-axis) and lower (y-axis) bound thresholds of the proposed model, θ_h and θ_l , respectively, when $k = 4$.

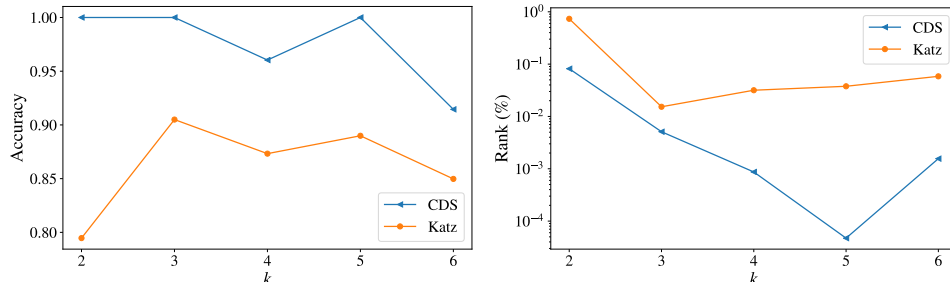


FIG. 9. Performance of the CDS method on the SBM in terms of the output’s accuracy (left) and rank (right), subject to changing budget size k (x-axis) when $\theta_l = 2, \theta_h = 2$.

a. Stochastic block model (SBM). Consider a relatively large network of size $n = 1000$, generated by a two-block SBM with different probabilities in the two communities, $p_1 = 0.015$ and $p_2 = 0.006$, and the connecting probability between the two being $p_{12} = 0.0005$. These values are chosen to maintain roughly the same mean degree as the SBM in Sec. VB 1, and we assign the same uniform weight $\alpha = 0.1$. We observe that the CDS method outperforms all the reference algorithms in all possible budget sizes; see Fig. 10. Further from the results, the performance of the degree centrality is similar to the Katz centrality, and we then prove that it is theoretically expected in Appendix D.

b. Collaboration network. The collaboration network is constructed by a comprehensive list of research papers in computer science provided by DBLP computer science bibliography, where two authors are connected if they publish at least one paper together [48]. There are intrinsic communities defined by the publication venue, e.g. journal or conference. Here, we select two such venues (no. 6035 and 6335) whose sizes are over 500 and the related authors are relatively densely connected so that the reinforcement within groups is more likely to happen. The resulting network is unweighted and connected, containing $n = 1016$ nodes and $|E| = 3469$ edges. Here, we maintain a uniform weight $\alpha = 0.1$. Since the collaboration network contains several nodes of much higher degrees than others, the performance of the linear dynamics is largely dominated by these nodes. Accordingly, we observe that both degree-centrality and Katz-centrality methods perform competitively to the CDS method when θ_l is relatively far from θ_h . However, the CDS method still outperforms others, and the

distance is relatively larger as θ_h becomes smaller; see Fig. 11.

VI. CONCLUSIONS

To understand how information propagates through social networks has many practical implications. Among the vast amount of work in this field, the IC model and the LT model are among the most popular choices of models. However, their characteristics, e.g. binary state variables and no feedback mechanism, while simplifying their analysis, neglect important mechanisms, e.g. a higher influence from people of higher activity and reinforcement within close-contact groups. Therefore, we extend both classic models to address these issues, and further propose a novel class of information propagation model unifying them. More importantly, the proposed model has features that each single model does not possess but may occur in real systems, as discussed in Sec. III (see Appendix B 1 for more details). We leave the investigation on real social networks to future work.

The general features of the proposed model necessarily lead to the IM problem with more general properties, such as the objective not being submodular. However, breaking the boundary of such restrictive properties is necessary for the IM problem to embrace a wider family of information propagation models in practice [21, 49]. Therefore, we introduce MINLP to the IM problem, and provide derivative-free methods as general solutions. Furthermore, we propose the CDS method particularly suited for the IM problem with the proposed model, and show its close-to-optimal performance in various scenar-

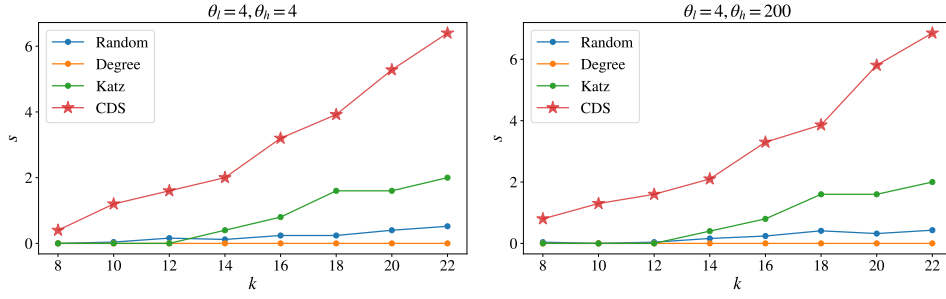


FIG. 10. Overall influence s from different node selection algorithms applied to the SBM, subject to changing budget size (x-axis), when the proposed information propagation model has $\theta_l = \theta_h = 4$ (left) and $\theta_l = 4, \theta_h = 200$ (right).

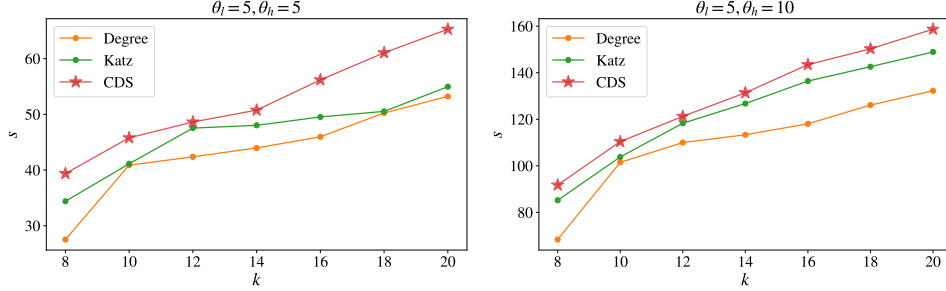


FIG. 11. Overall influence from different node selection algorithms applied to the collaboration network, subject to changing budget size (x-axis), when the proposed information propagation model has $\theta_l = \theta_h = 5$ (left) and $\theta_l = 5, \theta_h = 10$ (right), where the results from random sampling is ignored because they are always close to 0.

ios through experiments. One can also consider fine tuning each step as possible extensions to further improve the performance.

In summary, in this paper, we have unified the mechanisms underlying the IC model and the LT model into a novel class of information propagation model, and propose a general framework for the IM problem that is applicable to a broad range of functions describing the overall influence. As the two classic models are widely accepted for information propagation, we believe that the proposed model has the potential to explain more propagation phenomena on, but not restricted to, social networks. Meanwhile, the proposed IM framework provides a systematic approach to handle the case when the objective does not have desired properties (e.g. submodularity), which provides insights into solving the IM problem in more realistic scenarios.

ACKNOWLEDGMENTS

Y.T. is funded by the EPSRC Centre for Doctoral Training in Industrially Focused Mathematical Modelling (EP/L015803/1) in collaboration with Tesco PLC. R.L. acknowledges support from the EPSRC Grants EP/V013068/1 and EP/V03474X/1. We also thank Sebastian Lautz, Alisdair Wallis, Karel Devriendt, and London Roberts for useful discussions.

Appendix A: Proofs

1. Proofs for Sec. III

Proof of Lemma 1. We note that when a node v_j has $\sum_i W_{ij}x_i(t-1) > 0$, $\exists v_i \in V$ s.t. $x_i(t-1)W_{ij} > 0$. Then

$$\sum_i W_{ij}x_i(t-1) \geq wx_*(t-1),$$

where $x_*(t-1) = \min\{x_i(t-1) : x_i(t-1) > 0\}$. Hence, we can show that statement (6) is true by proving

$$wx_*(t-1) \geq l_{\min,0}w^t, \quad \forall t > 0,$$

by induction. (i) When $t = 1$, $x_*(0) \geq l_{\min,0}$, thus $wx_*(0) \geq l_{\min,0}w$. (ii) Suppose that $wx_*(t-1) \geq l_{\min,0}w^t$ is true $\forall t \leq t'$. Then when $t = t' + 1$, by the proposed model (2), for each node v_j with $x_j(t') > 0$,

$$\begin{aligned} x_j(t') &= f_{j,t'}\left(\sum_i W_{ij}x_i(t'-1)\right) \geq f_{j,t'}(wx_*(t'-1)) \\ &\geq f_{j,t'}(l_{\min,0}w^{t'}) = l_{\min,0}w^{t'}, \end{aligned}$$

where the first inequality is obtained by $f_{j,t'}(\cdot)$ being a non-decreasing function, the second one is obtained together with the induction hypothesis, and the equality at the end is because $l_{j,t} \leq l_{\min,0}w^t \leq h_{j,t}, \forall t > 0, v_j \in V$. Therefore, $wx_*(t') \geq wl_{\min,0}w^{t'} = l_{\min,0}w^{t'+1}$. \square

Proof of Theorem 2. We show that given such bounds in the proposed model (2),

$$\mathbf{x}(t)^T = \mathbf{x}(0)^T \mathbf{W}^t, \quad \forall t > 0, \quad (\text{A1})$$

by induction. By Lemma 1, there is no threshold effect from the current lower bounds, thus we will only check the saturation effect at the upper bounds in the following.

(i) When $t = 1$, for each node v_j , $\mathbf{x}(0)^T \mathbf{W}_{:,j} \leq h_{\max,0} \mathbf{1}^T \mathbf{W}_{:,j} \leq h_{j,1}$, since $x_i(0) \leq h_{\max,0}$ and $W_{ij} \geq 0$, $\forall i, j$. Hence, $x_j(1) = f_{j,1}(\mathbf{x}(0)^T \mathbf{W}_{:,j}) = \mathbf{x}(0)^T \mathbf{W}_{:,j}$, and $\mathbf{x}(1)^T = \mathbf{x}(0)^T \mathbf{W}$.

(ii) Suppose $\mathbf{x}(t)^T = \mathbf{x}(0)^T \mathbf{W}^t$, $\forall t \leq t'$. Then, for each node v_j

$$\begin{aligned} \mathbf{x}(t')^T \mathbf{W}_{:,j} &= \mathbf{x}(0)^T \mathbf{W}_{:,j}^{t'+1} \\ &\leq h_{\max,0} \mathbf{1}^T \mathbf{W}_{:,j}^{t'+1} \leq h_{j,t'+1}, \end{aligned}$$

where the equality is by the induction hypothesis, and the first inequality is again by $x_i(0) \leq h_{\max,0}$ and $W_{ij} \geq 0$, $\forall i, j$. Hence, $x_j(t'+1) = f_{j,t'+1}(\mathbf{x}(0)^T \mathbf{W}_{:,j}^{t'+1}) = \mathbf{x}(0)^T \mathbf{W}_{:,j}^{t'+1}$, and

$$\mathbf{x}(t'+1)^T = \mathbf{x}(0)^T \mathbf{W}^{t'+1}.$$

It is then straightforward to show that the dynamics characterised by (A1) has updating function (4) of the linear dynamics. \square

Proof of Claim 1. For the SBM, $\mathbf{W} = \alpha \mathbf{A}$, where \mathbf{A} is the (unweighted) adjacency matrix, and for each pair of nodes v_i, v_j , $A_{ij} \sim \text{Bernoulli}(p_{ij})$, with

$$p_{ij} = p_{in} \delta(\sigma_i, \sigma_j) + p_{out}(1 - \delta(\sigma_i, \sigma_j)),$$

where $\sigma_i \in \{1, 2\}$ indicates the block membership of each node v_i , and $\delta(i, j)$ is the delta function where $\delta(i, j) = 1$ if and only if $i = j$ and 0 otherwise. Further, we denote the linear part of the state vector by $\mathbf{y}(t+1) = \mathbf{W}^T \mathbf{x}(t)$, then for each node v_j at each time $t > 0$,

$$\begin{aligned} x_j(t) &= f_{j,t}(y_j(t)), \\ y_j(t) &= \sum_i W_{ij} x_i(t-1) = \alpha \sum_i A_{ij} x_i(t-1). \end{aligned}$$

Then at $t = 1$ [50],

$$\begin{aligned} y_j(1) &= \alpha \sum_i A_{ij} x_i(0) = \alpha l_0 \sum_{v_i \in \mathcal{A}_0} A_{ij} = \alpha l_0 \left(\sum_{v_i \in \mathcal{A}_0 \cap \mathcal{B}_{\sigma_j}} \text{Bernoulli}(p_{in}) + \sum_{v_i \in \mathcal{A}_0 \setminus \mathcal{B}_{\sigma_j}} \text{Bernoulli}(p_{out}) \right) \\ &= \alpha l_0 (\text{Bin}(k_{\sigma_j}, p_{in}) + \text{Bin}(k - k_{\sigma_j}, p_{out})), \end{aligned}$$

where $\mathcal{A}_0 = \{v_i : x_i(0) > 0\}$ is the (given) set of initially activated nodes, $k = |\mathcal{A}_0|$, and $k_i = |\mathcal{A}_0 \cap \mathcal{B}_i|$, $i = 1, 2$.

Hence, in case (i),

$$y_j(1) = \alpha l_0 (\text{Bin}(2, p_{in}) \delta(\sigma_j, 1) + \text{Bin}(2, p_{out}) \delta(\sigma_j, 2)),$$

while in case (ii),

$$y_j(1) = \alpha l_0 (\text{Bin}(1, p_{in}) + \text{Bin}(1, p_{out})).$$

When $l_{j,1} \leq l_1^*$, $x_j(1) = y_j(1)$, $\forall v_j \in V$. Then, in case (i),

$$\mathbb{E} \left[\sum_j (1 - \gamma) x_j(1) \right] = (1 - \gamma) n_b \times \alpha l_0 \times (2p_{in} + 2p_{out}),$$

where n_b is the size of each community, and in case (ii),

$$\mathbb{E} \left[\sum_j (1 - \gamma) x_j(1) \right] = 2(1 - \gamma) n_b \times \alpha l_0 \times (p_{in} + p_{out}).$$

Hence, the expected influence values at step 1 are the same in the two cases.

However, when $\alpha l_0 = l_1^* < l_{j,1} \leq 2l_1^* = 2\alpha l_0$, in case (i),

$$\begin{aligned} P(y_j(1) \geq l_{j,1}) &= P(y_j(1) = 2\alpha l_0) \\ &= P(\text{Bin}(2, p_{in}) \delta(\sigma_j, 1) + \text{Bin}(2, p_{out}) \delta(\sigma_j, 2) = 2) \\ &= p_{in}^2 \delta(\sigma_j, 1) + p_{out}^2 \delta(\sigma_j, 2), \end{aligned}$$

thus,

$$\begin{aligned} &\mathbb{E} \left[\sum_j (1 - \gamma) x_j(1) \right] \\ &= (1 - \gamma) \left(\sum_j 0 P(y_j(1) < l_{j,1}) + 2\alpha l_0 P(y_j(1) = 2\alpha l_0) \right) \\ &= (1 - \gamma) n_b \times 2\alpha l_0 \times (p_{in}^2 + p_{out}^2). \end{aligned} \quad (\text{A2})$$

While, in case (ii),

$$\begin{aligned} P(y_j(1) \geq l_{j,1}) &= P(y_j(1) = 2\alpha l_0) \\ &= P(\text{Bin}(1, p_{in}) + \text{Bin}(1, p_{out}) = 2) = p_{in} p_{out}, \end{aligned}$$

thus,

$$\begin{aligned} & \mathbb{E} \left[\sum_j (1 - \gamma) x_j(1) \right] \\ &= (1 - \gamma) \left(\sum_j 0P(y_i(1) < l_{j,1}) + 2\alpha l_0 P(y_j(1) = 2\alpha l_0) \right) \\ &= 2(1 - \gamma)n_b \times 2\alpha l_0 \times p_{in}p_{out}. \end{aligned} \quad (\text{A3})$$

Hence, the expectation from (i) as in (A2) is larger than the one from (ii) as in (A3) by condition (7). \square

Proof of Theorem 3. We first note that if (12) is true, then for each node $v_j \in V$,

$$\begin{aligned} \sum_{t=0}^{\infty} (1 - \gamma)^t x_j(t) &= \sum_{t=0}^{\infty} (1 - \gamma)^t (\theta_l \alpha)^t x'_j(t) \\ &= \sum_{t=0}^{\infty} (1 - \gamma)^t x'_j(t), \end{aligned}$$

thus the network has the same overall influence from the two models.

We then show that (12) is true by induction on the time step t . (i) At $t = 0$, $x_j(0) = (\theta_l \alpha)^0 x'_j(0)$, since $x_j(0) = x'_j(0)$, $\forall v_j \in V$. (ii) Suppose $x_j(t) = (\theta_l \alpha)^t x'_j(t)$, $\forall v_j \in V$, is true for all $t \leq t'$, then for each node v_j at $t = t' + 1$, if we denote $y_j(t' + 1) = \sum_i W_{ij} x_i(t')$,

$$x_j(t' + 1) = \begin{cases} 0, & y_j(t' + 1) < l_{j,t'+1}, \\ y_j(t' + 1), & l_{j,t'+1} \leq y_j(t' + 1) < h_{j,t'+1}, \\ h_{j,t}, & y_j(t' + 1) \geq h_{j,t'+1}, \end{cases} \quad (\text{A4})$$

where $l_{j,t'+1} = (\theta_l \alpha)^{t'+1}$ and $h_{j,t'+1} = \theta_h \theta_l^{t'} \alpha^{t'+1} h_{j,0}$, by the proposed model (2). We now consider the state value $x'_j(t' + 1)$ from model (10) in the three different cases, and compare it with the state value $x_j(t + 1)$ in (A4). (1) When

$$\begin{aligned} & \sum_i W_{ij} x_j(t') < l_{j,t'+1} = (\theta_l \alpha)^{t'+1} \\ \Leftrightarrow & \sum_i W_{ij} (\theta_l \alpha)^{t'} x'_i(t') < (\theta_l \alpha)^{t'+1} \\ \Leftrightarrow & \sum_i W_{ij} x'_j(t' + 1) < \theta_l \alpha = l'_j, \end{aligned}$$

we have $(\theta_l \alpha)^{t'+1} x'_j(t' + 1) = 0 = x_j(t' + 1)$.

(2) When

$$\begin{aligned} & \sum_i W_{ij} x_j(t) \geq h_{j,t'+1} = \theta_h \theta_l^{t'} \alpha^{t'+1} h_{j,0} \\ \Leftrightarrow & \sum_i W_{ij} (\theta_l \alpha)^{t'} x'_i(t') \geq \theta_h \theta_l^{t'} \alpha^{t'+1} h_{j,0} \\ \Leftrightarrow & \sum_i W_{ij} x'_j(t') \geq \theta_h \alpha h_{j,0} = h'_j, \end{aligned}$$

we then have $(\theta_l \alpha)^{t'+1} x'_j(t' + 1) = (\theta_l \alpha)^{t'+1} m_j = (\theta_l \alpha)^{t'+1} (\theta_h h_{j,0}) / \theta_l = h_{j,t'+1} = x_j(t' + 1)$.
(3) Finally, in the remaining case when

$$\begin{aligned} l_{j,t'+1} &\leq \sum_i W_{ij} x_j(t) < h_{j,t'+1} \\ \Leftrightarrow l'_j &\leq \sum_i W_{ij} x'_j(t' + 1) < h'_j, \end{aligned}$$

the state value is in the linear regime where

$$\begin{aligned} x'_j(t' + 1) &= \frac{m_j - 1}{h'_j - l'_j} \left(\sum_i W_{ij} x'_j(t') - l'_j \right) + 1 \\ &= \frac{(\theta_h h_{j,0}) / \theta_l - 1}{\theta_h \alpha h_{j,0} - \theta_l \alpha} \left(\sum_i W_{ij} x'_j(t') - \theta_l \alpha \right) + 1 \\ &= \frac{1}{\theta_l \alpha} \sum_i W_{ij} x'_j(t') = \frac{1}{\theta_l \alpha} \sum_i W_{ij} \frac{1}{(\theta_l \alpha)^{t'}} x_j(t') \\ &= \frac{1}{(\theta_l \alpha)^{t'+1}} \sum_i W_{ij} x_j(t') = \frac{1}{(\theta_l \alpha)^{t'+1}} x_j(t' + 1). \end{aligned}$$

Hence, we have shown that $x_j(t' + 1) = (\theta_l \alpha)^{t'+1} x'_j(t' + 1)$, $\forall v_j \in V$. \square

Proof of Claim 2. Since the underlying network has uniform weight α , $\mathbf{W} = \alpha \mathbf{A}$. (1) When $\theta_h = \theta_l > 1$, $x_i(t') = (\theta_l \alpha)^t l_0$, $\forall v_i \in \mathcal{A}_{t'}$. Then we have

$$\sum_i W_{ij_*} x_i(t') = \alpha (\theta_l \alpha)^t l_0 < \theta_l \alpha (\theta_l \alpha)^t l_0 = l_{j_*,t'+1},$$

thus node v_{j_*} cannot have positive state value at $t' + 1$.
(2) When $\theta_h > \theta_l > 1$, the highest possible value of node j_0 at time t' is $\theta_h \theta_l^{t'-1} \alpha^{t'} l_0$. Hence, node v_{j_*} can have positive state value at $t' + 1$ if

$$\begin{aligned} W_{j_0 j_*} \theta_h \theta_l^{t'-1} \alpha^{t'} l_0 &\geq l_{j_*,t'+1} \\ \Leftrightarrow \alpha \theta_h \theta_l^{t'-1} \alpha^{t'} l_0 &\geq (\theta_l \alpha)^{t'+1} l_0 \\ \Leftrightarrow \theta_h &\geq \theta_l^2, \end{aligned}$$

which can be achieved given that θ_h is sufficiently large. \square

2. Proofs for Sec. IV

Proof of Theorem 5. By Lemma 1, the lower bounds are effectively 0. Therefore, in the proposed model (2), $f_{j,t}(x) = 0$ if and only if $x = 0$, $\forall v_j \in V$, $t > 0$. Hence, $f_{j,t}(x)$ is equivalent to another bound function $\tilde{f}_{j,t}(x)$ associated with the same upper bound $\tilde{h}_{j,t} = h_{j,t}$ but a different lower bound $\tilde{l}_{j,t} = 0$.

We first note that if $f_{j,t}(x)$ is continuous for all $v_j \in V$ and $t > 0$, then by the properties of composite continuous functions, the objective function $s(\cdot)$ is also continuous.

Now, we focus on $f_{j,t}(x)$, and show that it is continuous by proving the continuity of $\tilde{f}_{j,t}(x)$. (1) There are two parts of the function that are always continuous, i.e. when $\tilde{l}_{j,t} < x < \tilde{h}_{j,t}$ and $x > \tilde{h}_{j,t}$. (2) We can show that the function is also continuous at the boundary points, where

$$\lim_{x \rightarrow \tilde{h}_{j,t}^-} \tilde{f}_{j,t}(x) = \tilde{h}_{j,t} = \tilde{f}_{i,t}(\tilde{h}_{j,t}) = \lim_{x \rightarrow \tilde{h}_{j,t}^+} \tilde{f}_{j,t}(x),$$

and

$$\lim_{x \rightarrow \tilde{l}_{j,t}^+} \tilde{f}_{j,t}(x) = 0 = \tilde{f}_{j,t}(\tilde{l}_{j,t}).$$

Hence, $\tilde{f}_{j,t}(x)$ is continuous for all $x \geq 0$.

Then for the concavity, we note that if $f_{j,t}(x)$ is concave for all $v_j \in V$ and $t > 0$, then since it is also non-decreasing (and the linear function $h(\mathbf{x}) = \mathbf{W}^T \mathbf{x}$ is also concave and nondecreasing), the objective function $s(\cdot)$ is concave by the properties of composite concave functions. Now, we consider specifically $\tilde{f}_{j,t}(x)$, and show that it is concave by the concavity of $\tilde{f}_{j,t}(x)$, i.e. $\forall x, y \geq 0$ and $\beta \in [0, 1]$,

$$\tilde{f}_{j,t}((1 - \beta)x + \beta y) \geq (1 - \beta)\tilde{f}_{j,t}(x) + \beta\tilde{f}_{j,t}(y). \quad (\text{A5})$$

(1) When $0 = \tilde{l}_{j,t} \leq x, y < \tilde{h}_{j,t}$ or $x, y \geq \tilde{h}_{j,t}$, (A5) is true by the concavity of linear functions and constant functions, respectively.

(2) When $\tilde{l}_{j,t} \leq x < \tilde{h}_{j,t} \leq y$, $\tilde{f}_{j,t}(x) = x < \tilde{h}_{j,t}$ and $\tilde{f}_{j,t}(y) = \tilde{h}_{j,t} \leq y$. Then, if $(1 - \beta)x + \beta y \geq \tilde{h}_{j,t}$,

$$\begin{aligned} \tilde{f}_{j,t}((1 - \beta)x + \beta y) &= \tilde{h}_{j,t} \\ &= (1 - \beta)\tilde{h}_{j,t} + \beta\tilde{f}_{j,t}(y) \\ &\geq (1 - \beta)\tilde{f}_{j,t}(x) + \beta\tilde{f}_{j,t}(y); \end{aligned}$$

otherwise $(1 - \beta)x + \beta y < \tilde{h}_{j,t}$,

$$\begin{aligned} \tilde{f}_{j,t}((1 - \beta)x + \beta y) &= (1 - \beta)x + \beta y \\ &= (1 - \beta)\tilde{f}_{j,t}(x) + \beta y \\ &\geq (1 - \beta)\tilde{f}_{j,t}(x) + \beta\tilde{f}_{j,t}(y). \end{aligned}$$

(3) When $\tilde{l}_{j,t} \leq y < \tilde{h}_{j,t} \leq x$, (A5) is true by exchanging x, y in case (2). Hence, $\tilde{f}_{j,t}(x)$ is concave for all $x \geq 0$. \square

Proof of Theorem 6. By Theorem 2, the proposed model reaches the linear-dynamics extreme. Then as in (16), the objective function $s(\cdot)$ is linear in \mathbf{x} where

$$s(\mathbf{x}) = \mathbf{c}^T \mathbf{x},$$

where $\mathbf{c} = ((\mathbf{I} - (1 - \gamma)\mathbf{W})^{-1} - \mathbf{I})\mathbf{1}$. For illustrative purposes, we split the proof into two parts. (1) We first analyse the MINLP (15) solely w.r.t. \mathbf{x} while fixing the

integer variables \mathbf{z} . It can then be decomposed into n sub-problems, where for each $v_j \in V$,

$$\begin{aligned} \max_{x_j} \quad & \tilde{s}_j(x_j) := c_j x_j \\ \text{s.t.} \quad & x_j \leq h_{j,0} z_j, \\ & x_j \geq l_{j,0} z_j, \\ & x_j \in \mathbb{R}. \end{aligned} \quad (\text{A6})$$

Because $c_j, z_j \geq 0$, $\forall v_j \in V$, we can show that the optimal solution to each sub-problem (A6) is $x_j^* = h_{j,0} z_j$, and the optimal value is $\tilde{s}_j^* = c_j h_{j,0} z_j$. (2) Then we consider the MINLP (15) w.r.t. \mathbf{z} when \mathbf{x} is at its optimal value, where

$$\begin{aligned} \max_{\mathbf{z}} \quad & \sum_j \tilde{s}_j^* = \sum_j c_j h_{j,0} z_j \\ \text{s.t.} \quad & \sum_j z_j \leq k, \\ & z_j \in \{0, 1\}, \forall j. \end{aligned}$$

We can show that the optimal solution is to set $z_j = 1$ if node j is ranked among the top k according to its coefficient in the objective, $c_j h_{j,0}$. This gives the solution in (17). \square

Appendix B: Further features of the proposed model

In this section, we discuss other interesting features of the proposed model in Sec. III. We first show that both the locally linear-dynamics-like and the locally linear-threshold-like propagation can co-exist in a single network in Sec. B 1, and then numerically analyse this feature in Sec. B 2. We conclude with a discussion of the derivative information of the overall influence w.r.t. the initial states in Sec. B 3, which plays an important role in the IM problem in Sec. IV.

1. Coexistence of regimes

As discussed in Sec. III, an important feature of the proposed model is that it can be reduced to the linear dynamics at one end and the extended LT model at the other. Here, we show that both types of propagation can coexist in a single network given that the underlying propagation process follows the proposed model, which further illustrates the generality in the proposed model.

Specifically, we construct a network as in Fig. 12, where we connect a tree, composed by nodes $\cup_{i=1, i \neq 7}^{11} \{v_i\} \cup \{v_{12}, v_{13}, v_{15}, v_{16}, v_{17}, v_{21}\}$, and part of a regular lattice, composed by nodes $\{v_6, v_7, v_8, v_{13}, v_{14}, v_{15}, v_{18}, v_{19}, v_{20}\}$. Suppose we activate the nodes in red initially. Then (1) if the underlying propagation is perfectly linear, every nodes will have positive state values as soon as possible, while (2) if the propagation follows the extended LT

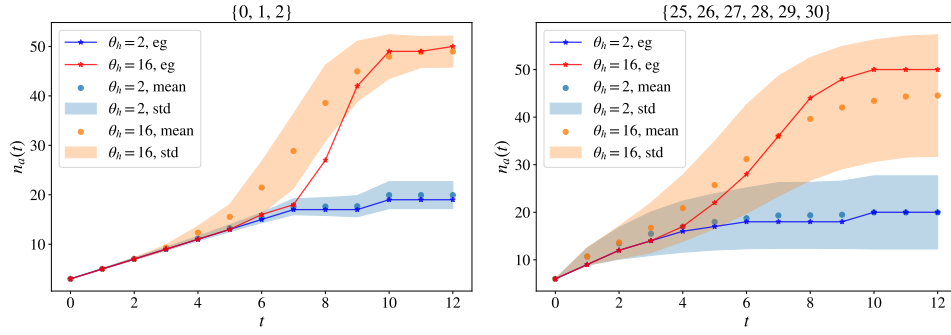


FIG. 14. The number of nodes of positive (weighted) sum of state values up to increasing time steps (x-axis), from the extended LT model ($\theta_l = \theta_h = 2$) and from a general case in the proposed model ($\theta_l = 2, \theta_h = 16$), with the initially activated nodes in the regular lattice (left) and the ER random part (right), where “eg” shows the results on the composite network in Fig. 13 and others are from the results on 1000 samples of the random composite network.

We observe that, particularly clearly in the composite network in Fig. 13, the set from either part of the network can eventually influence the whole network from the general case of the proposed model, while only certain parts of the network can be reached from the extended LT model; see Fig. 14. The two propagation processes initially proceed similarly in terms of the number of nodes with $s_j(t) > 0$, while after this “initial preparation” phase, the general case of the proposed model gradually reaches more nodes and finally the whole network. The results are generally consistent with those obtained from 1000 samples from the random composite network. Since the randomness is mostly from the ER model part, the number of nodes with $s_j(t) > 0$ has more variance when the initially activated nodes are from this part.

3. Derivative and backpropagation

To understand how the overall influence change w.r.t. the initial state values is important in many applications, e.g. the influence maximisation problem we consider in Sec. IV. With a functional form for the proposed model at each time step, we can then analyse the derivative information though *backpropagation* or *chain rule* given the influence function is differentiable, for this purpose.

Now, we slice the overall influence along the dimension of time, and consider the influence at each time step t ,

$$s_t(\mathbf{x}(0)) = \sum_j (1 - \gamma)^t x_j(t), \quad (\text{B1})$$

where

$$s(\mathbf{x}(0)) = \sum_{t=1}^{\infty} s_t(\mathbf{x}(0)).$$

Following the proposed model, $s_t(\mathbf{x}(0))$ can be considered as the output of a *neural network*, with t hidden layers, $\mathbf{x}(0)$ as the input layer, \mathbf{W}^T as the weight matrix and $\{f_{j,t'}\}$ as the activation functions for nodes $\{v_j\}$ in the

layers corresponding to $t' = 1, 2, \dots, t$. The output layer only consists of one node, and is computed by summing over the elements in the previous layer corresponding to $\mathbf{x}(t) = (x_j(t))$.

We first note that s_t is not always differentiable, and even discontinuous in the general form, because each bound function $f_{j,r}$ can have jump discontinuity at $l_{j,r}$ and be non-differentiable at $h_{j,r}$ at each time step $r \leq t$. However, $f_{j,r}$ is always semi-differentiable, specifically right-differentiable, with the right derivative,

$$\partial_+ f_{j,r}(x) = \begin{cases} 1, & l_{j,r} \leq x < h_{j,r}, \\ 0, & x < l_{j,r}, x \geq h_{j,r}, \end{cases} \quad (\text{B2})$$

thus so is the function s_t , by the chain rule of semi-differentiability and $W_{ij} > 0, \forall i, j$. Therefore, we can obtain the right derivative of s_t with respect to $\mathbf{x}(0)$, $\partial_+ s_t = (\partial_+ s_t(x_i(0)))$, where if we denote $\mathbf{y}(r) = \mathbf{W}^T \mathbf{x}(r-1)$, and $\partial_+ \mathbf{f}_r = (\partial_+ f_{j,r}(y_j(r)))$, $\forall r \leq t$, we have

$$\frac{1}{(1 - \gamma)^t} \partial_+ s_t^T = \partial_+ \mathbf{f}_t^T \frac{\partial \mathbf{y}(t)}{\partial \mathbf{x}(t-1)} \prod_{r=1}^{t-1} \mathbf{Diag}(\partial_+ \mathbf{f}_r) \frac{\partial \mathbf{y}(r)}{\partial \mathbf{x}(r-1)},$$

where ∂ is the (bidirectional) derivative, $\partial \mathbf{y} / \partial \mathbf{x} = (\partial y_i / \partial x_j)$ with $\mathbf{x}, \mathbf{y} \in \mathbb{R}^n$, and $\mathbf{Diag}(\cdot)$ is the corresponding diagonal matrix. Here, $\partial \mathbf{y}(t) / \partial \mathbf{x}(t-1) = \mathbf{W}^T$, $\forall t > 0$, thus the right derivative can be reduced to

$$\frac{1}{(1 - \gamma)^t} \partial_+ s_t^T = \partial_+ \mathbf{f}_t^T \mathbf{W}^T \prod_{r=1}^{t-1} \mathbf{Diag}(\partial_+ \mathbf{f}_r) \mathbf{W}^T. \quad (\text{B3})$$

From Eq. (B2), $\partial_+ f_{j,r}(\cdot) \in \{0, 1\}$, $\forall v_j \in V, r > 0$, hence the overall right derivative in (B3) is a restricted version of the (bidirectional) derivative in the case of the corresponding linear dynamics where $\partial f_{j,r}(\cdot) = 1$, $\forall v_j \in V, r > 0$, and

$$\frac{1}{(1 - \gamma)^t} \partial_+ s_t^T = \mathbf{1}^T (\mathbf{W}^T)^t. \quad (\text{B4})$$

Therefore, the right derivative can be useful if the propagation is dominated by the linear part, but will almost always be 0 if the lower bounds are close to the upper bounds. Suppose at a particular time step t' , $l_{j,t'} = h_{j,t'} = l_{t'}$, $\forall v_j \in V$, then $f_{j,t'}(x) = l_{t'}H(x - l_{t'})$, where $H(\cdot)$ is the Heaviside step function, and

$$\frac{df_{j,t'}(x)}{dx} = l_{t'} \frac{dH(x - l_{t'})}{dx} = l_{t'}\delta(x - l_{t'}), \quad (\text{B5})$$

where $\delta(x)$ is the *Dirac delta function* with $\delta(x) = +\infty$ if $x = 0$ and 0 otherwise. Accordingly, the derivative $\partial s_t(x_j(0))$ for each node v_j at any time steps $t \geq t'$ can only be 0 or $+\infty$, which is not very informative. We conclude here that the derivative information generally has limited use in understanding the change of the overall influence, and accordingly in the IM problem.

Appendix C: Further features of the influence maximisation

In this section, we discuss more details of the influence maximisation problem. We first explore the constraint of limited budget size in Sec. C1. Then we give more details of the general MADS approach in Sec. C2 and the experiments exploring the performance of the proposed CDS method in Sec. C3. Finally, we discuss the time complexity of the proposed method in Sec. C4. As in Sec. V, $l_{j,0} = h_{j,0} = 1$, $\forall v_j \in V$, $\gamma = 0$, and we apply exclusively the threshold-type bounds in (9) with condition (11).

1. Budget size

We start from exploring the dependence of the optimal objective value on the budget size k , through small networks, because it is practically hard for global algorithms like the brute-force to obtain an optimal solution in large networks.

Specifically, we consider a network of $n = 20$ nodes, generated from a two-block SBM with connecting probability $p_1 = 0.5$ in one community, $p_2 = 0.25$ in the other, and $p_{12} = 0.05$ between the two communities. The probabilities in the two communities are set to be different in order to separate the nodes in each community. We again assign uniform weight $\alpha = 0.1$, and consider different bound values by varying θ_l, θ_h . We compare objective values s^* obtained with different budget sizes through the *relative optimal objective value*, s^*/s_{max}^* , where s_{max}^* is the optimal value from $k = n = 20$, i.e. the maximum objective value with respect to all possible k .

We observe that the optimal objective value reaches its maximum level at a smaller budget size k , as the upper bounds decrease; see Fig. 15. When $\theta_l = \theta_h = 2$, only activating $k = 11$ nodes initially can achieve the maximum level of influence on the network, and for $\theta_l = \theta_h = 1$, only $k = 6$ nodes are needed. This property of saturation

also illustrates the rationality for the IM problem where one aims to influence a large portion of the network from a small set of initially activated nodes: it is not only because of limited resource, but also that activating more nodes does not necessarily benefit the optimisation substantially.

Interestingly, when enlarging the lower bounds, the early-saturation characteristics is not significant, but the step effect is increasingly explicit; see Fig. 16. When $\theta_l = \theta_h$, the optimal objective function changes as a step function with respect to the budget size k , and when $\theta_l = 1$, it is closer to being linear. When θ_l lies in between these two extremes, the optimal objective function interpolates these two shapes, with both linear-like increase and step effect, consistently with the proposed model capturing features both from the linear dynamics and the extended LT model.

2. MADS method

We now discuss in more detail the method that the proposed CDS method for the influence maximisation problem is largely based on: the MADS method.

In the MADS for mixed variables (MV), each vector $\mathbf{y} = (\mathbf{y}^c, \mathbf{y}^d)$ is partitioned into its continuous and discrete components, and we denote the maximum dimensions of the continuous and discrete variables by n^c and n^d respectively, thus $\mathbf{y}^c \in \Omega^c \subseteq \mathbb{R}^{n^c}$ and $\mathbf{y}^d \in \Omega^d \subseteq \mathbb{Z}^{n^d}$. The general problem [51] under consideration is given by

$$\min_{\mathbf{y} \in \Omega} f(\mathbf{y}),$$

where $f : \Omega \rightarrow \mathbb{R} \cup \{\infty\}$, and the domain, or the feasible region, is the union of continuous domain across possible discrete variable values, i.e.

$$\Omega = \bigcup_{\mathbf{y}^d \in \Omega^d} (\Omega^c(\mathbf{y}^d) \times \{\mathbf{y}^d\}),$$

where $\Omega^c(\mathbf{y}^d)$ indicates that the continuous domain can change with different discrete variable values, and $\Omega = \Omega^c$ if $n^d = 0$. The constraints are incorporated in the domain, and are treated by the extreme barrier approach f_Ω , where $f_\Omega(\mathbf{y}) = f(\mathbf{y})$ if $\mathbf{y} \in \Omega$ and ∞ otherwise.

MADS is a local search methods, which aims to find a *local minimiser* as defined in Def. 2. As discussed in Sec. IV B, one common choice for integer variables is $\mathcal{N}(\mathbf{y}) = \{\mathbf{y}' \in \Omega : \mathbf{y}'^c = \mathbf{y}^c, \|\mathbf{y}'^d - \mathbf{y}^d\|_1 \leq 1\}$.

Definition 2. A point $\mathbf{y} = (\mathbf{y}^c; \mathbf{y}^d) \in \Omega$ is said to be a *local minimiser* of a function f on Ω with respect to the set of neighbours $\mathcal{N}(\mathbf{y}) \subset \Omega$ if there exists an $\epsilon > 0$ such that $f(\mathbf{y}) \leq f(\tilde{\mathbf{y}})$ for all $\tilde{\mathbf{y}}$ in the set

$$\Omega \cap \left(\bigcup_{\mathbf{y}' \in \mathcal{N}(\mathbf{y})} B_\epsilon(\mathbf{y}'^c) \times \mathbf{y}'^d \right),$$

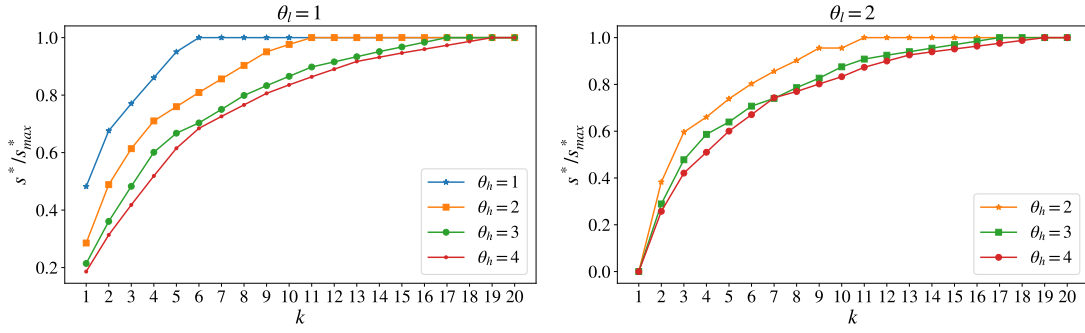


FIG. 15. The change of relative optimal objective value s^*/s_{max}^* with respect to the budget size k (x-axis) on the SBM, when the proposed model has varying upper bound threshold θ_h while the lower bound threshold $\theta_l = 1$ (left) and $\theta_l = 2$ (right).

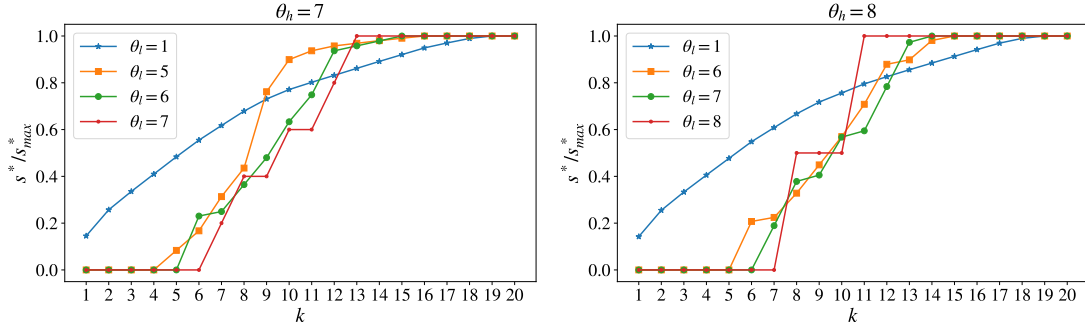


FIG. 16. The change of relative optimal objective value s^*/s_{max}^* with respect to the budget size k (x-axis) from the SBM, when the proposed model has varying lower bound threshold θ_l while the upper bound threshold $\theta_h = 7$ (left) and $\theta_h = 8$ (right).

where $B_\epsilon(\mathbf{y}^c) = \{\mathbf{y}' \in \mathbb{R}^{n^c} : \|\mathbf{y}' - \mathbf{y}^c\| < \epsilon\}$ with $\epsilon > 0$ is an open ball, and $\mathcal{N}(\mathbf{y})$ is a user-defined discrete neighbourhood.

MADS algorithm is characterised by an optional **search** step, a local **poll** step, and an **extended poll** step, where the objective f_Ω is evaluated at specific points defined on an underlying mesh M_r at each iteration r . The goal of each iteration is to find a feasible improved mesh point from current iterate, $\mathbf{y} \in M_r$ s.t. $f_\Omega(\mathbf{y}) < f_\Omega(\mathbf{y}^{(r)})$, and the algorithm will output the point it converges to. The mesh M_r at each iteration r is a central concept in the method, which is formed as the direct product of Ω^d with the union of a finite number of lattices in Ω^c ,

$$M_r = \bigcup_{q=1}^{q_{max}} M_r^q \times \Omega^d, \quad (\text{C1})$$

where $q = 1, \dots, q_{max}$ indicates each combination of discrete variable values, and the lattice M_r^q is defined through previously evaluated points, the positive spanning directions and the mesh size parameter Δ_r^m which dictates its coarseness. In the **poll** step, the method evaluates the discrete neighbourhood $\mathcal{N}(\mathbf{y}^{(r)})$, and the points whose continuous part is close to the current iterate along certain directions, $P_r(\mathbf{y}^{(r)})$, controlled by Δ_r^m and the poll size parameter Δ_r^p . The **extended poll**

step is triggered when the **poll** step fails to find an improved point. It consists of a finite sequence of **poll** steps performed around the points in $\mathcal{N}(\mathbf{y}^{(r)})$ whose objective value is sufficiently close to the incumbent value, i.e. $f_\Omega(\mathbf{y}^{(r)}) \leq f_\Omega(\mathbf{y}) \leq f_\Omega(\mathbf{y}^{(r)}) + \xi_r$, for some user-defined tolerance $\xi_r \geq \xi$ (e.g. $\xi_r = \max\{\xi, 0.05|f(\mathbf{y}^{(r)})|\}$), and we denote such set of nodes by $\mathcal{N}_r^{\xi_r}(\mathbf{y}^{(r)})$. We summarise the main ideas of MADS in Alg. 3.

3. The CDS method

Here, we provide the further details from analysing the performance of the CDS method on both real and synthetic networks of various structures, to complement the results in Sec. V B 1. Here, we maintain the same setting as in Sec. V.

a. Karate club network. The karate club network is a social network of a university karate club [52]. It captures $n = 34$ members of the club, and has $|E| = 78$ edges indicating pairs of members who interact outside the club. This real network is comprehensively used in network analysis for various purposes, while in a manageable small scale, thus is suitable here.

Algorithm 3 Mesh adaptive direct search for mixed variables (MADS-MV).

- 1: Initialisation: Set $\xi > 0$ and $\xi_0 \geq \xi$. Let $\mathbf{y}^{(0)} \in \Omega$ such that $f_\Omega(\mathbf{y}^{(0)}) < \infty$, set $\Delta_0^p \geq \Delta_0^m > 0$. Set iteration $r = 0$.
 - 2: **SEARCH** step (optional): Evaluate f_Ω on a finite set of trial points on the mesh M_r (C1). If an improved mesh point is found, the **SEARCH** step may terminate, skip the next **POLL** step and go directly to step 5.
 - 3: **POLL** step: Evaluate f_Ω on the set $P_r(\mathbf{y}^{(r)}) \cup \mathcal{N}(\mathbf{y}^{(r)}) \subset M_r$ (i.e. close to the current iterate), until an improved mesh point is found, or until all points have been exhausted. If an improved mesh point is found, go to step 5.
 - 4: **EXTENDED POLL** step: Perform a finite sequence of **poll** step starting from each point $\mathbf{y} \in \mathcal{N}_r^{\xi_r}(\mathbf{y}^{(r)}) \subseteq \mathcal{N}(\mathbf{y}^{(r)})$ with $f_\Omega(\mathbf{y}^{(r)}) \leq f_\Omega(\mathbf{y}) \leq f_\Omega(\mathbf{y}^{(r)}) + \xi_r$, until an improved mesh point is found or until all points have been exhausted.
 - 5: Parameter update: Coarsen Δ_{r+1}^m and Δ_{r+1}^p when an improved mesh point is found and refine them otherwise. Update $\xi_r \geq \xi$, increment $r \leftarrow r + 1$, and go to step 2.
-

When $k = 3$, the CDS method can successfully find an optimal solution in all different choices of the upper and lower bounds; see Fig. 17. Furthermore, the time consumed by the CDS method is always less than 5% of the brute-force’s which is between 1s and 4s.

We then change the budget size k in two different cases of bounds: (i) $\theta_l = 2$, $\theta_h = 16$, and (ii) $\theta_l = 2 = \theta_h$, the extended LT model. We observe that the CDS method can always find a global optimal solution in case (i), while the performance drops slightly as k increases but is still close-to-optimal in case (ii); see Fig. 18. Moreover, the time consumption of the CDS method increases approximately linearly as k rises, while for the brute-force, it changes exponentially, which makes it practically hard to obtain a global optimum under larger budget sizes.

b. Composite network. The composite network here particularly refers to the one in Fig. 13, constructed by connecting a regular lattice of size $n_o = 25$ and mean degree $d_o = 4$, and a ER random graph of the same size n_o and probability $p_{er} = d_o/n$, with edges randomly placed between the two parts by a small probability $p_o = 0.01$. As discussed in Appendix B 2, there is noticeable difference in performance between the extended LT model and a general case of the proposed model in this network. It is then interesting to explore the performance of the CDS method for the corresponding IM task, on this particular structure.

When $k = 4$, the CDS method can again find an optimal or close-to-optimal solution with different choices of the upper and lower bound thresholds: see Fig. 19. There are only 4 cases where the CDS method cannot output a globally optimal solution, and the worst-case scenario occurs when $\theta_l = 1.4$ and $\theta_h = 2$, with accuracy about 0.85 and rank slightly below 0.009% in overall 230, 300 possibly initially activated sets, i.e. the CDS method can output a top 20 set in this case.

Since there are certain cases where a global optimum

cannot be reached by the plain CDS method, we explore one improvement strategy here: to restart the search process, i.e. steps 2,3,4 in Alg. 2, from other unexplored points. We achieve this by its noticeable community structure (see [53] for theoretical results on the interplay between the community structure and complex contagions). Specifically, we propose the following *community restart strategy*: (i) construct a set containing different splits of k into the two communities, $\mathcal{S} := \{(k_1, k_2) : k_1 + k_2 = k, k_1, k_2 \in \mathbb{N}\}$; (ii) construct the set of initial points corresponding to activating k_1 and k_2 nodes of the highest values of $h_{j,0}c_j$ where c_j is the Katz centrality of node v_j , in communities 1 and 2, respectively, $\forall (k_1, k_2) \in \mathcal{S}$; (iii) restart the search process from each point in (ii) if it is has not been explored yet. We observe that the community restart strategy can assist the CDS method to find a global optimum when the lower bound threshold $\theta_l < 2$; see Fig. 8. Now, the worst-case scenario has accuracy 0.98 and rank 0.001%, i.e. it can now output a top 2 set.

We then explore the performance of the CDS method, together with the community restart strategy, when varying the budget size k and $\theta_l = 1.4, \theta_h = 2$, the pair with worst-case performance when $k = 4$. The performance of the CDS method is generally good, with accuracy greater than 0.8 and consistently low rank, and the performance can be further improved by the community restart strategy, particularly when k is large; see Fig. 20. The results also verifies the valuable information in the community structure.

4. Time complexity of the CDS method

Finally, we discuss the time complexity of the proposed CDS method, through decomposing it into two parts: (I) the evaluation of the objective function, and (II) the number of evaluations required until convergence. From Theorem 4, we know that given a network, the worst-case scenario of (I) occurs when the proposed model reduces to the linear dynamics, since it corresponds to an achievable upper bound for t_ϵ . Hence, the CDS method circumvents the worst-case complexity by starting from the solution associated with the linear dynamics. For (II), we further decompose it into the product of (i) the size of discrete neighbourhood that is feasible, and roughly, (iia) the number of steps towards convergence, or more precisely, (iib) the number of evaluations divided by the neighbourhood size. (i) is $k(n - k)$, by Eq. (19) and Eq. (20), and is equivalently $O(n)$ since k is normally assumed to be $O(1)$. The only remaining part for a full description of the time complexity is (iia) or (iib), both are related to the rate of convergence which is difficult to provide a theoretical guarantee given the general properties of the objective function. Instead, we conjecture that the complexity of (iib) does not increase significantly when varying the network size n , i.e. approximately $O(1)$, given the same mean degree, and verify it

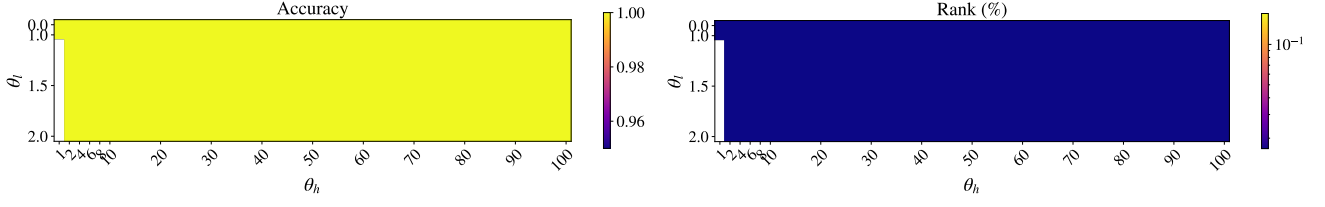


FIG. 17. Performance of the CDS method on the karate club network in terms of the output’s accuracy (left) and the rank (%), subject to changing upper (x-axis) and lower (y-axis) bound thresholds of the proposed model, θ_h and θ_l , respectively, when $k = 3$.

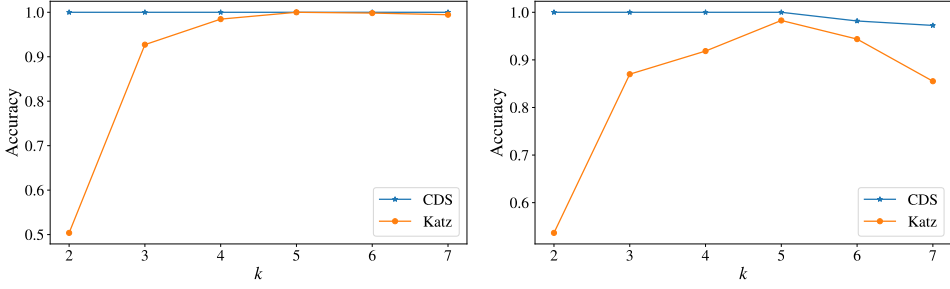


FIG. 18. Performance of the CDS method on the Karate club network in terms of the output’s accuracy, subject to changing budget size k (x-axis) when $\theta_l = 2, \theta_h = 16$ (left) and $\theta_l = \theta_h = 2$ (right).

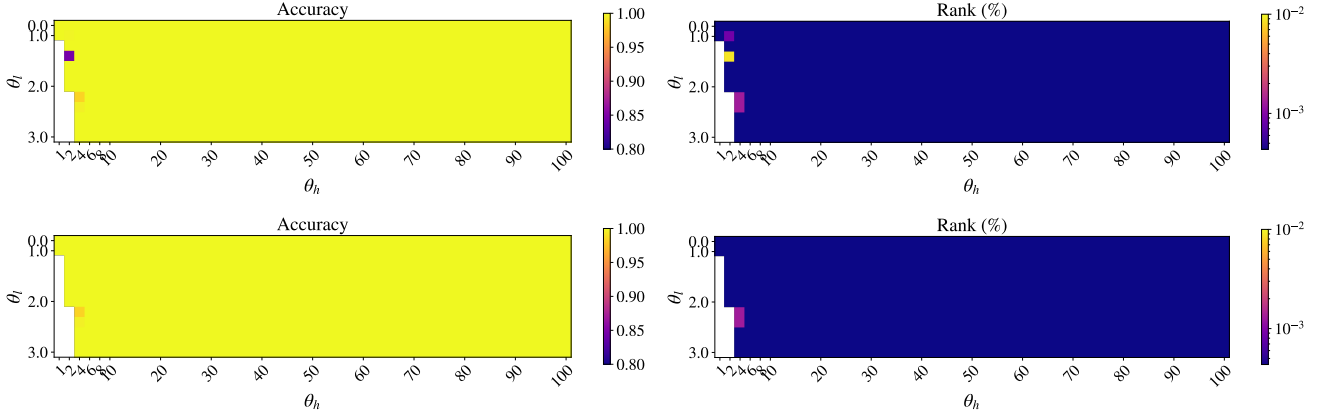


FIG. 19. Performance of the CDS method (top) and that with community restart (bottom) on the composite network in terms of the output’s accuracy (left) and the rank (%), subject to changing upper (x-axis) and lower (y-axis) bound thresholds of the proposed model, θ_h and θ_l , respectively, when $k = 4$.

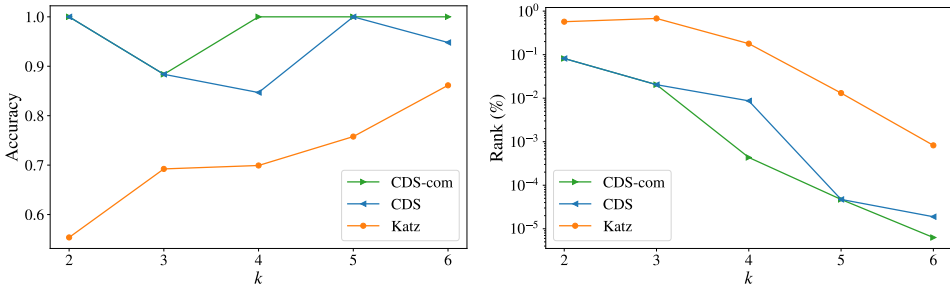


FIG. 20. Performance of the CDS method (“CDS”) and that with community restart (“CDS-com”) on the composite network in terms of the output’s accuracy (left) and rank (right), subject to changing budget size k (x-axis) when $\theta_l = 1.4, \theta_h = 2$.

empirically through experiments in ER random graphs.

Specifically, we construct ER random graphs of the same expected node degree, $\langle d \rangle = (n-1)p$ where n is the network size and p is the connecting probability in ER graphs, but of increasing size n . We then apply the CDS method to the IM problem on this series of graphs to explore the dependence of its time complexity on the network size n . The experiments are performed with different combinations of parameters in order to take into account their effects, including the upper bounds, the lower bounds, and the budget size k . Here, we assign uniform weight $\alpha = 0.1$ to all the networks, set $l_{j,0} = h_{j,0} = 1$, $\forall v_j \in V$, $\gamma = 0$, and apply exclusively the threshold-type bounds in (9) with condition (11), as in Sec. V.

Overall, the time increases linearly when the network is small, and once the network size reaches a critical value, the increase slows down; see Fig. 21 for $k = 3$ and Fig. 22 for $k = 5$, with different combinations of parameters (θ_l, θ_h) . Having different mean degree, upper bounds, lower bounds, or budget sizes normally causes shifts in the trends but not the overall shape.

We now integrate the experiment results with the theoretical understanding. For (I), we know from Alg. 1 that only neighbours of currently positive nodes are considered when calculating the state value in the next step. Since we maintain the same mean degree in our setting, the difference in time lies in t_ϵ which is at least $O(1)$. For (iia), the size of the feasible discrete neighbourhood $n(n-k)$ increases linearly in n , and we also note that when $\theta_l > 1$ only including nodes sharing common neighbours with other initially activated nodes can improve the overall influence, which is also applied in the algorithm (in refining the mesh at each time step) to reduce the complexity to be lower than $O(n)$. From the experiments, we observe linear increase, and also the increase slows down significantly after certain critical value of n . Therefore, it is reasonable to conjecture that (iib), the number of evaluations required by the CDS method divided by the feasible neighbourhood size, is approximately $O(1)$ in the IM problem in real networks.

These all together result in the value of (II) to be approximately $O(n)$. To measure the goodness of this complexity value, we compare it with a global algorithm, the brute-force method, where each node set will be evaluated. Then, overall $\binom{n}{k}$ evaluations are needed, which is proportional to $O(n^k)$ since again $k = O(1)$. Therefore, $O(n^{k-1})$ more multiples of evaluations are needed in the global algorithm than the CDS method.

The time complexity of the CDS method can be further improved by parallel programming, although it is described in Alg. 2 and currently performed serially. For instance, the tasks to evaluate the objective function of different candidates in a discrete neighbourhood can be run in parallel. There are also other optimisation techniques to further reduce the complexity, e.g. coarse evaluation of the objective function with a higher tolerance at early stage. All these can be included in future work.

Appendix D: SBM

In this section, we discuss the properties of SBMs mentioned in the main text in more detail. We first show that when increasing the upper bounds, the increase in the expected influence from the node set in one community is higher than the other evenly distributed in the two communities, as in Sec. III C 2, and then prove that a node is expected to have higher Katz centrality if it has higher degree centrality than others, as in Sec. V B 2.

Claim 3. *With $l_{j,0} = h_{j,0} = l_0$, and $l_{j,1} = 2\alpha l_0$, $\forall v_j \in V$, if SBM(p_{in}, p_{out}) of two equally-sized [54] communities, $\mathcal{B}_1, \mathcal{B}_2$, and uniform weight α satisfies*

$$p_{in} > p_{out}, \quad (1 - p_{in}) > p_{out}, \quad (\text{D1})$$

or

$$p_{out} > p_{in}, \quad (1 - p_{out}) > p_{in}, \quad (\text{D2})$$

then when $h_{j,1}$ rises from $h_{j,1} = l_{j,1} = 2\alpha l_0$ to $h_{j,1} = 2l_{j,1} = 4\alpha l_0$, $\forall v_j \in V$, the increase in the expected influence, $\mathbb{E}[\sum_j (1-\gamma)x_j(1)]$, from the initially activated node set (i) $\mathcal{A}_0 = \{v_{i_1}, v_{i_2}, v_{i_3}, v_{i_4}\} \subset \mathcal{B}_1$, is larger than that from (ii) $\mathcal{A}_0 = \{v_{j_1}, v_{j_2}, v_{j_3}, v_{j_4} : v_{j_1}, v_{j_2} \in \mathcal{B}_1, v_{j_3}, v_{j_4} \in \mathcal{B}_2\}$.

Proof. For the SBM, $\mathbf{W} = \alpha \mathbf{A}$, where \mathbf{A} is the (unweighted) adjacency matrix. We maintain the same notations for the block membership of each node v_i , $\sigma_i \in \{1, 2\}$, the linear part of the state vector, $\mathbf{y}(t+1) = \mathbf{W}^T \mathbf{x}(t)$, and the size of each community n_b , as in the proof of Claim 1 in Appendix A 1.

In case (i),

$$y_j(1) = \alpha l_0 (\text{Bin}(4, p_{in}) \delta(\sigma_j, 1) + \text{Bin}(4, p_{out}) \delta(\sigma_j, 2)),$$

while in case (ii),

$$y_j(1) = \alpha l_0 (\text{Bin}(2, p_{in}) + \text{Bin}(2, p_{out})).$$

When $h_{j,1} = l_{j,1} = 2\alpha l_0$, $\forall v_j \in V$,

$$\begin{aligned} & \mathbb{E} \left[\sum_j x_j(1) \right] \\ &= \sum_j 0P(y_j(1) < l_{j,1}) + 2\alpha l_0 P(y_j(1) \geq 2\alpha l_0). \end{aligned} \quad (\text{D3})$$

When $h_{j,1} = 4\alpha l_0$, $\forall v_j \in V$,

$$\begin{aligned} & \mathbb{E} \left[\sum_j x_j(1) \right] \\ &= \sum_j (0P(y_j(1) < l_{j,1}) + 2\alpha l_0 P(y_j(1) = 2\alpha l_0) \\ & \quad + 3\alpha l_0 P(y_j(1) = 3\alpha l_0) + 4\alpha l_0 P(y_j(1) = 4\alpha l_0)). \end{aligned} \quad (\text{D4})$$

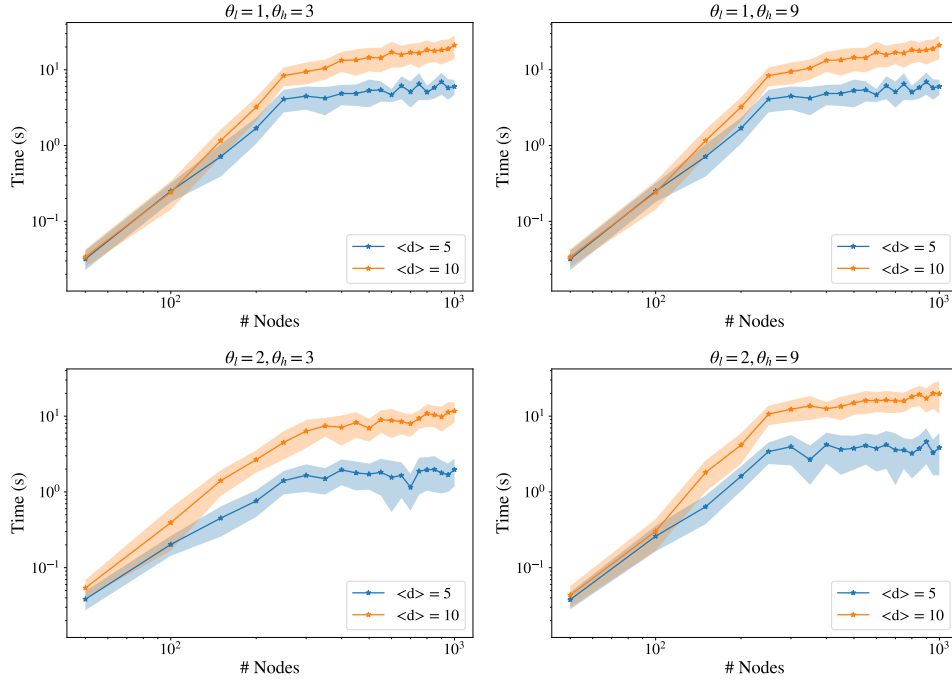


FIG. 21. Time consumption of the CDS method on ER random graphs of increasing sizes (x-axis) when $k = 3$, where we consider different combinations of parameters (θ_l, θ_h) while maintaining the same mean degree 5 (blue) and 10 (orange), on 50 samples of the ER graphs of each size n , with dots showing the mean value and shades indicating the standard deviation.

Hence, the increase in the expected influence, ignoring the factor $1 - \gamma$, is the difference between the two equations (D4) and (D3), i.e.

$$\Delta = \sum_j \alpha l_0 P(y_j(1) = 3\alpha l_0) + 2\alpha l_0 P(y_j(1) = 4\alpha l_0).$$

In case (i),

$$\begin{aligned} \Delta_{(i)} &= \sum_j \alpha l_0 \left(\binom{4}{3} p_{in}^3 (1 - p_{in}) \delta(\sigma_j, 1) + \binom{4}{3} p_{out}^3 (1 - p_{out}) \delta(\sigma_j, 2) \right) + 2\alpha l_0 (p_{in}^4 \delta(\sigma_j, 1) + p_{out}^4 \delta(\sigma_j, 2)) \\ &= n_b \times \alpha l_0 \times 2 (2p_{in}^3 (1 - p_{in}) + 2p_{out}^3 (1 - p_{out}) + p_{in}^4 + p_{out}^4). \end{aligned}$$

While in case (ii),

$$\begin{aligned} \Delta_{(ii)} &= \sum_j \alpha l_0 \left(\binom{2}{1} p_{in} (1 - p_{in}) p_{out}^2 + p_{in}^2 \binom{2}{1} p_{out} (1 - p_{out}) \right) + 2\alpha l_0 (p_{in}^2 p_{out}^2) \\ &= 2n_b \times \alpha l_0 \times (2p_{in}^2 p_{out} (1 - p_{out}) + 2p_{out}^2 p_{in} (1 - p_{in}) + 2p_{in}^2 p_{out}^2). \end{aligned}$$

Hence,

$$\begin{aligned} \Delta_{(i)} - \Delta_{(ii)} &= 2n_b \alpha l_0 (2(p_{in}^2 - p_{out}^2)(p_{in}(1 - p_{in}) - p_{out}(1 - p_{out})) \\ &\quad + (p_{in}^2 - p_{out}^2)^2), \end{aligned}$$

which is positive given condition (D1) or (D2). \square

Theorem 7. In a two-block SBM with the connecting

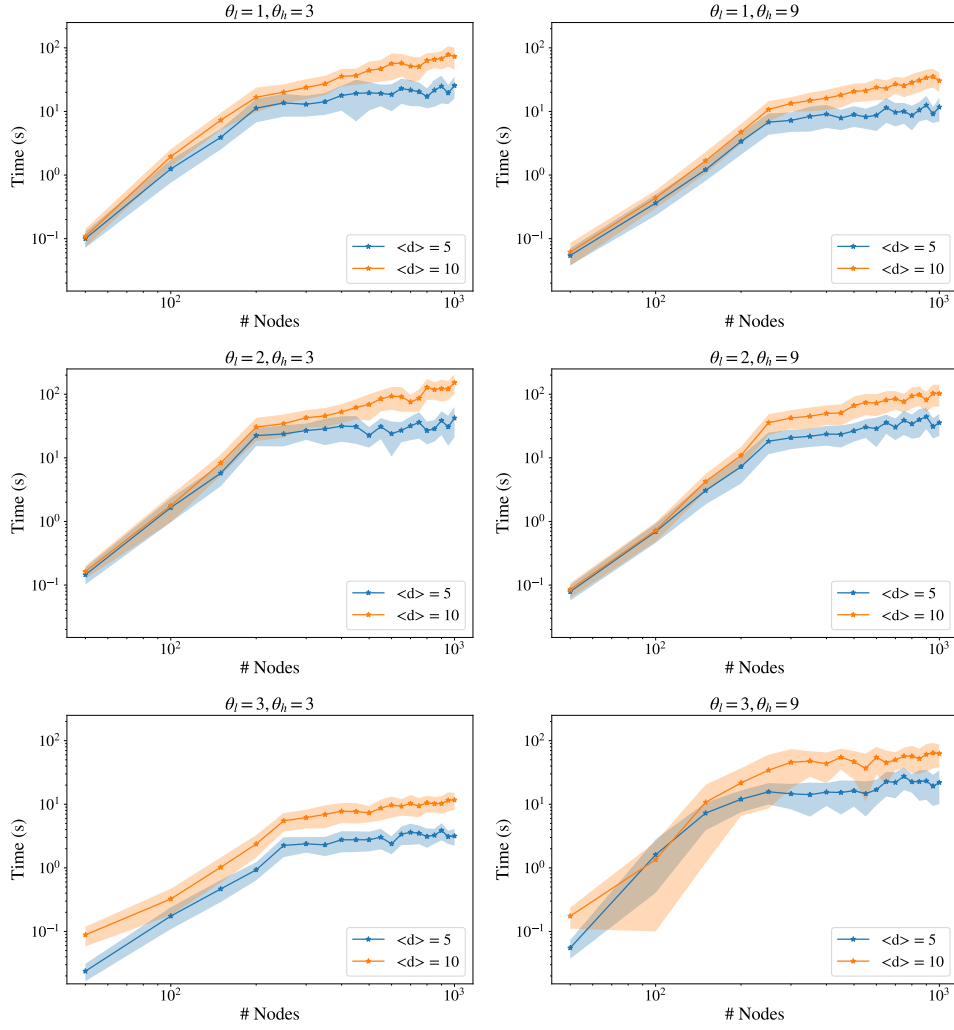


FIG. 22. Time consumption of the CDS method on ER random graphs of increasing sizes (x-axis) when $k = 5$, where we consider different combinations of parameters (θ_l, θ_h) while maintaining the same mean degree 5 (blue) and 10 (orange), on 50 samples of the ER graphs of each size n , with dots showing the mean value and shades indicating the standard deviation.

probabilities in the two communities, $\mathcal{B}_1, \mathcal{B}_2$, being p_1, p_2 , respectively, and between the two being p_{12} , if a node v_i is expected to have higher degree centrality than another node v_j ,

$$\mathbb{E} \left[\sum_r A_{ir} \right] > \mathbb{E} \left[\sum_r A_{jr} \right], \quad (\text{D5})$$

where $\mathbf{A} = (A_{ij})$ is the adjacency matrix, then node v_i is expected to have higher Katz centrality than node v_j ,

$$\mathbb{E} \left[\sum_{t=1}^{\infty} \alpha_{\text{katz}}^t \sum_r A_{ri}^t \right] > \mathbb{E} \left[\sum_{t=1}^{\infty} \alpha_{\text{katz}}^t \sum_r A_{rj}^t \right], \quad (\text{D6})$$

where α_{katz} is the discounting factor.

Proof. In such SBM, for each pair of nodes v_i, v_j , A_{ij} is an independently distributed Bernoulli random variable, with success probability p_1 if $v_i, v_j \in \mathcal{B}_1$, p_2 if $v_i, v_j \in \mathcal{B}_2$,

and p_{12} otherwise. Hence, nodes in the same communities are equivalent, and there are only two distinct expected values in both centralities, one for each community.

For the degree centrality [55],

$$\mathbb{E} \left[\sum_r A_{ir} \right] = \begin{cases} n_1 p_1 + n_2 p_{12}, & v_i \in \mathcal{B}_1, \\ n_1 p_{12} + n_2 p_2, & v_i \in \mathcal{B}_2, \end{cases}$$

where n_1, n_2 are the sizes of communities $\mathcal{B}_1, \mathcal{B}_2$, respectively. Hence, condition (D5) can only happen when nodes v_i and v_j are in different communities.

Without loss of generality, we assume $v_i \in \mathcal{B}_1$, and then $v_j \in \mathcal{B}_2$. We show that (D6) holds true by proving the following stronger relationship where for each $t > 0$,

$$\mathbb{E} \left[\sum_r A_{ri}^t \right] > \mathbb{E} \left[\sum_r A_{rj}^t \right]. \quad (\text{D7})$$

We show it by induction on t . (i) When $t = 1$,

$$\begin{aligned} \mathbb{E} \left[\sum_r A_{ri} \right] &= n_1 p_1 + n_2 p_{12} \\ &> n_1 p_{12} + n_2 p_2 = \mathbb{E} \left[\sum_r A_{rj} \right], \end{aligned}$$

where the inequality is by condition (D5). (ii) Suppose (D7) is true for all $t \leq t'$. Then when $t = t' + 1$,

$$\begin{aligned} &\mathbb{E} \left[\sum_r A_{ri}^{t'+1} \right] \tag{D8} \\ &= \mathbb{E} \left[\sum_r \sum_q A_{rq}^{t'} A_{qi} \right] \\ &= \sum_{v_q \in \mathcal{B}_1} \mathbb{E} \left[\sum_r A_{rq}^{t'} \right] p_1 + \sum_{v_q \in \mathcal{B}_2} \mathbb{E} \left[\sum_r A_{rq}^{t'} \right] p_{12} \\ &= \mathbb{E} \left[\sum_r A_{ri}^{t'} \right] n_1 p_1 + \mathbb{E} \left[\sum_r A_{rj}^{t'} \right] n_2 p_{12}, \tag{D9} \end{aligned}$$

where the second equality is by independence, and the last equality is by equivalence among nodes in the same communities. Similarly,

$$\mathbb{E} \left[\sum_r A_{rj}^{t'+1} \right] = \mathbb{E} \left[\sum_r A_{ri}^{t'} \right] n_1 p_{12} + \mathbb{E} \left[\sum_r A_{rj}^{t'} \right] n_2 p_2. \tag{D10}$$

Hence, the difference (D9) - (D10) is

$$\begin{aligned} &\mathbb{E} \left[\sum_r A_{ri}^{t'} \right] n_1 (p_1 - p_{12}) + \mathbb{E} \left[\sum_r A_{rj}^{t'} \right] n_2 (p_{12} - p_2) \\ &> \mathbb{E} \left[\sum_r A_{rj}^{t'} \right] (n_1 (p_1 - p_{12}) + n_2 (p_{12} - p_2)) > 0, \end{aligned}$$

where the first inequality is by induction hypothesis, and the last inequality is by condition (D5). \square

-
- [1] E. Bakshy, I. Rosenn, C. Marlow, and L. Adamic, The role of social networks in information diffusion, in *Proceedings of the 21st International Conference on World Wide Web* (ACM, 2012) pp. 519–528.
- [2] D. Centola, The spread of behavior in an online social network experiment, *Science* **329**, 1194 (2010).
- [3] M. Nekovee, Y. Moreno, G. Bianconi, and M. Marsili, Theory of rumour spreading in complex social networks, *Phys. A* **374**, 457 (2007).
- [4] A. Bovet and H. Makse, Influence of fake news in twitter during the 2016 us presidential election, *Nat. Commun.* **10**, 10.1038/s41467-018-07761-2 (2019).
- [5] W. Chen, C. Wang, and Y. Wang, Scalable influence maximization for prevalent viral marketing in large-scale social networks, in *Proceedings of the 16th ACM SIGKDD International Conference on Knowledge Discovery and Data Mining* (ACM, 2010) pp. 1029–1038.
- [6] J. Leskovec, L. Adamic, and B. Huberman, The dynamics of viral marketing, *ACM Trans. Web* **1**, 5 (2007).
- [7] E. Mossel and S. Roch, Submodularity of influence in social networks: From local to global, *SIAM Journal on Computing* **39**, 2176 (2010).
- [8] R. Pastor-Satorras, C. Castellano, P. Van Mieghem, and A. Vespignani, Epidemic processes in complex networks, *Rev. Mod. Phys.* **87**, 925 (2015).
- [9] R. Pastor-Satorras and A. Vespignani, Epidemics in the internet, in *Evolution and Structure of the Internet: A Statistical Physics Approach* (Cambridge University Press, Cambridge, 2004) pp. 180–210.
- [10] D. Kempe, J. Kleinberg, and E. Tardos, Maximizing the spread of influence through a social network, in *Proceedings of the 9th ACM SIGKDD International Conference on Knowledge Discovery and Data Mining* (ACM, 2003) pp. 137–146.
- [11] P. Shakarian, A. Bhatnagar, A. Aleali, E. Shaabani, and R. Guo, The independent cascade and linear threshold models, in *Diffusion in Social Networks* (Springer International Publishing, Cham, 2015) pp. 35–48.
- [12] D. Centola and M. Macy, Complex contagions and the weakness of long ties, *Amer. J. Sociol.* **113**, 702 (2007).
- [13] D. Guilbeault, J. Becker, and D. Centola, Complex contagions: A decade in review, in *Complex Spreading Phenomena in Social Systems: Influence and Contagion in Real-World Social Networks* (Springer International Publishing, Cham, 2018) pp. 3–25.
- [14] H. Ma, H. Yang, M. Lyu, and I. King, Mining social networks using heat diffusion processes for marketing candidates selection, in *Proceedings of the 17th ACM Conference on Information and Knowledge Management* (ACM, 2008) pp. 233–242.
- [15] M. Degroot, Reaching a consensus, *J. Amer. Statist. Assoc.* **69**, 118 (1974).
- [16] G. Deffuant, D. Neau, F. Amblard, and G. Weisbuch, Mixing beliefs among interacting agents, *Adv. Complex Syst.* **03**, 87 (2000).
- [17] J. Leskovec, A. Krause, C. Guestrin, C. Faloutsos, J. VanBriesen, and N. Glance, Cost-effective outbreak detection in networks, in *Proceedings of the 13th ACM SIGKDD International Conference on Knowledge Discovery and Data Mining* (ACM, 2007) pp. 420–429.
- [18] X. Song, B. Tseng, C. Lin, and M. Sun, Personalized recommendation driven by information flow, in *Proceedings of the 29th Annual International ACM SIGIR Conference on Research and Development in Information Retrieval* (ACM, 2006) pp. 509–516.
- [19] A. Goyal, W. Lu, and L. Lakshmanan, Celf++: Optimizing the greedy algorithm for influence maximization in social networks, in *Proceedings of the 20th In-*

- ternational Conference Companion on World Wide Web* (ACM, 2011) pp. 47–48.
- [20] S. Banerjee, M. Jenamani, and D. Pratihari, A survey on influence maximization in a social network, *Knowledge Inf. Syst.* **62**, 3417 (2020).
- [21] Y. Li, J. Fan, Y. Wang, and K. Tan, Influence maximization on social graphs: A survey, *IEEE Trans. Knowledge Data Engrg.* **30**, 1852 (2018).
- [22] P. Belotti, C. Kirches, S. Leyffer, J. Linderoth, J. Luedtke, and A. Mahajan, Mixed-integer nonlinear optimization, *Acta Numer.* **22**, 1 (2013).
- [23] F. Boukouvala, R. Misener, and C. Floudas, Global optimization advances in Mixed-Integer Nonlinear Programming, MINLP, and Constrained Derivative-Free Optimization, *CDFO, European J. Oper. Res.* **252**, 701 (2016).
- [24] S. Burer and A. N. Letchford, Non-convex mixed-integer nonlinear programming: A survey, *Surv. Oper. Res. Manag. Sci.* **17**, 97 (2012).
- [25] M. Abramson, C. Audet, J. Chrissis, and J. Walston, Mesh adaptive direct search algorithms for mixed variable optimization, *Optim. Lett.* **3**, 35 (2009).
- [26] W. Chen, C. Castillo, and L. Lakshmanan, *Information and Influence Propagation in Social Networks* (Morgan & Claypool, 2013).
- [27] C. Borgs, M. Brautbar, J. Chayes, and B. Lucier, Maximizing social influence in nearly optimal time, in *Proceedings of the 25th Annual ACM-SIAM Symposium on Discrete Algorithms* (SIAM, 2014) pp. 946–957.
- [28] W. Chen, Y. Yuan, and L. Zhang, Scalable influence maximization in social networks under the linear threshold model, in *2010 IEEE International Conference on Data Mining* (IEEE, 2010) pp. 88–97.
- [29] C. Wang, W. Chen, and Y. Wang, Scalable influence maximization for independent cascade model in large-scale social networks, *Data Min. Knowl. Discov.* **25**, 545 (2012).
- [30] N. Chen, On the approximability of influence in social networks, *SIAM J. Discrete Math.* **23**, 1400 (2009).
- [31] D. Kempe, J. Kleinberg, and E. Tardos, Maximizing the spread of influence through a social network, *Theory Comput.* **11**, 105 (2015).
- [32] E. Even-Dar and A. Shapira, A note on maximizing the spread of influence in social networks, in *Internet and Network Economics*, edited by X. Deng and F. Graham (Springer Berlin Heidelberg, 2007) pp. 281–286.
- [33] P. Dubey, R. Garg, and B. De Meyer, Competing for customers in a social network: The quasi-linear case, in *Internet and Network Economics* (Springer Berlin Heidelberg, Berlin, Heidelberg, 2006) pp. 162–173.
- [34] M. Grabisch, A. Mandel, A. Rusinowska, and E. Tanimura, Strategic influence in social networks, *Math. Oper. Res.* **43**, 29– (2018).
- [35] E. Demaine, M. Hajiaghayi, H. Mahini, D. Malec, S. Raghavan, A. Sawant, and M. Zadimoghadam, How to influence people with partial incentives, in *Proceedings of the 23rd International Conference on World Wide Web* (ACM, 2014) pp. 937–948.
- [36] V. Srivastava, J. Moehlis, and F. Bullo, On bifurcations in nonlinear consensus networks, in *Proceedings of the 2010 American Control Conference* (IEEE, 2010) pp. 1647–1652.
- [37] M. Asllani, T. Carletti, F. Di Patti, D. Fanelli, and F. Piazza, Hopping in the crowd to unveil network topology, *Phys. Rev. Lett.* **120**, 158301 (2018).
- [38] D. Fanelli and A. McKane, Diffusion in a crowded environment, *Phys. Rev. E* **82**, 021113 (2010).
- [39] In the specific case here, the upper bound $2l_1^*$ is equivalent to require that at most two initially activated neighbours are needed to activate a node.
- [40] Z. Lu, W. Zhang, W. Wu, J. Kim, and B. Fu, The complexity of influence maximization problem in the deterministic linear threshold model, *J. Comb. Optim.* **24**, 374 (2012).
- [41] L. Vicente and A. Custódio, Analysis of direct searches for discontinuous functions, *Math. Program.* **133**, 299 (2012).
- [42] C. Audet, L. D. S., V. Montplaisir, and C. Tribes, NOMAD version 4: Nonlinear optimization with the MADS algorithm, preprint [arXiv:2104.11627v2](https://arxiv.org/abs/2104.11627v2) (2021).
- [43] S. Le Digabel, Algorithm 909: Nomad: Nonlinear optimization with the mads algorithm, *ACM Trans. Math. Software* **37**, 10.1145/1916461.1916468 (2011).
- [44] M. Laguna, F. Gortázar, M. Gallego, A. Duarte, and R. Martí, A black-box scatter search for optimization problems with integer variables, *J. Global Optim.* **58**, 497 (2014).
- [45] T. Giovannelli, G. Liuzzi, S. Lucidi, and F. Rinaldi, Derivative-free methods for mixed-integer nonsmooth constrained optimization, preprint [arXiv:2107.00601](https://arxiv.org/abs/2107.00601) (2021).
- [46] Note that as long as the probabilities satisfy $p_{in} > p_{out}$, the similar phenomena will occur.
- [47] M. Newman, The structure of scientific collaboration networks, *Proc. Natl. Acad. Sci.* **98**, 404 (2001).
- [48] J. Yang and J. Leskovec, Defining and evaluating network communities based on ground-truth, *Knowl. Inf. Syst.* **42**, 181 (2015).
- [49] F. Gursoy and D. Gunec, Influence maximization in social networks under deterministic linear threshold model, *Knowledge-Based Systems* **161**, 111 (2018).
- [50] Note that the expressions of initially activated nodes can be different from others in the same community, due to the common assumption of no self-edges. However, we assume $k \ll n$ where $n = |V|$ is the number of nodes, thus ignore such differences.
- [51] Note the general MADS method considers the minimisation problem, therefore we transform our objective to be $\min_{\mathbf{x}, \mathbf{z}} -F(\mathbf{x})$ when applying the algorithm.
- [52] W. Zachary, An information flow model for conflict and fission in small groups, *J. Anthropol. Res.* **33**, 452 (1977).
- [53] G. Schoenebeck, B. Tao, and F. Yu, Think globally, act locally: On the optimal seeding for nonsubmodular influence maximization, in *Approximation, Randomization, and Combinatorial Optimization. Algorithms and Techniques (APPROX/RANDOM 2019)* (Schloss Dagstuhl–Leibniz-Zentrum fuer Informatik, 2019) pp. 39:1–39:20.
- [54] Note the same results can be obtained with arbitrary community sizes, but extra conditions on both the community sizes and the probabilities are required.
- [55] Note that the expected values could be slightly different due to the common assumption of no self-edges. However, we assume $n \gg 1$, thus ignore such differences.